NL82C0763

MONTE CARLO SIMULATION OF RADIATIVE PROCESSES IN ELECTRON-POSITRON SCATTERING

$e^+ e^- \rightarrow \mu \mu \gamma$

QED

R.H.P. KLEISS

MONTE CARLO SIMULATION
OF RADIATIVE PROCESSES
IN ELECTRON-POSITRON
SCATTERING

Promotor: Prof. Dr. F.A. Berends

Referenten: Prof. Dr. K.J.F. Gaemers
             Dr. R. Gastmans

γιά τίς τρεῖς
μικρούλες μού

CONTENTS

6

CHAPTER I

OUTLINE

In 1960 the first storage ring for colliding e^+e^- beams, with a circumference of about 4 metres, was built in Frascati. At CERN, experiments with the LEP machine, which has a circumference of more than 27 kilometres, should start at the end of the 80's. In the meantime, both the size and complexity of the experiments have grown with the same speed, resulting in new theoretical insights as well as an increasing need for methods to translate the theoretical predictions into experimentally meaningful quantities. The Monte Carlo simulation of scattering processes has turned out to be one of the most successful ways to do this.

It is the purpose of this thesis to describe how this approach can be applied to higher-order QED corrections to several fundamental processes. The outline of this work is as follows. In chapter II a very brief overview of the currently interesting phenomena in e^+e^- scattering is given. It is argued that accurate information on higher-order QED corrections is very important and that the Monte Carlo approach is one of the most flexible and general methods to obtain this information. In chapter III we describe various techniques which are useful in this context, and make a few remarks on the numerical aspects of the proposed method. In the following three chapters we apply this to the processes $e^+e^- \rightarrow \mu^+\mu^-(\gamma)$ and $e^+e^- \rightarrow q\bar{q}(\gamma)$. In chapter IV we motivate our choice of these processes in view of their experimental and theoretical relevance. We give the formulae necessary for a computer simulation of all quantities of interest, up to order α^3. In chapters V and VI we describe how this simulation can be performed using the techniques mentioned in chapter III. In chapter VII we show how additional dynamical quantities, namely the polarization of the incoming and outgoing particles, can be incorporated in our treatment, and we give the relevant formulae for the example processes mentioned above. Finally, in chapter VIII we present some examples of the comparison between theoretical predictions based on Monte Carlo simulations as outlined here, and the results from actual experiments.

CHAPTER II

INTRODUCTION

1. e^+e^- physics

Over the last decade many of the most important contributions to the
present-day understanding of elementary particles and their interactions have
come from experiments using colliding electron and positron beams. One very
obvious advantage of these experiments is that all the energy of the
colliding particles can be used to probe the interactions, in contrast to
experiments with only one beam, where only a small fraction of this energy
is available. Another one is that electrons and positrons are still pointlike
at even the highest available energies. Hence the collision products form a
clean signal as compared to collisions of hadrons, where many of the hadron
constituents do not interact and give a contamination of the final state.

As major qualitative successes e^+e^- scattering has established the
existence of two new quarks (c,b), a new lepton (τ) and a new type of gauge
boson (gluon). Important quantitative results have been the precision tests
of QED, the measurement of R (the ratio between the cross section for hadron
production and the one for muon pair production) and of the strong coupling
constant α_s, the development of quarkonium spectroscopy, achievements in
the field of 2γ physics, and a first determination of weak coupling constants
for a timelike momentum transfer [1].

It is outside the scope of this thesis to go into any detail about the
present status of e^+e^- physics. Apart from searches for new and/or unexpected
phenomena, the investigations center around the study of three fundamental
interactions, and the possible theories describing them:

1. electromagnetic interactions, described by
   - quantum electrodynamics (QED)

2. strong interactions, described by
   - quantum chromodynamics (QCD)
   - potential models for $q\bar{q}$ bound states
   - models for the quark structure of hadrons

3. weak interactions, described by
   - gauge models, all more or less similar to the "standard" model

8

(SU(2) × U(1) gauge theory of Glashow, Weinberg and Salam with broken gauge symmetry)

- different models for weak decays of hadrons.

Many reviews exist [1] that give detailed information about accomplishments and prospects in any of these fields. We will restrict ourselves to a feature common to all e^+e^- experiments, that is, the necessity of taking into account radiative corrections.

2. Radiative corrections

Since in any e^+e^- process at least two charged particles are involved, it is necessary to take into account the effect of the accompanying electromagnetic fields. Indeed, it has been shown [2] that the cross section for the scattering of "bare" charges, without any emission of electromagnetic radiation, is strictly speaking equal to zero.

Apart from the effects of vacuum polarization, radiative corrections are applied to a given process by letting an extra photon interact with the charged particles present in the reaction. This photon may be virtual (i.e. off mass shell) in which case it has to be emitted and absorbed during the interaction, giving rise to a final state which is identical to that of the lowest order process. In case it is real (massless), it will propagate into the final state and may be detected as bremsstrahlung. In this way radiative corrections affect all experimental distributions and it is necessary to include them in a careful analysis of e^+e^- scattering experiments.

On the other hand, radiative processes where hard bremsstrahlung is emitted may be studied in their own right, without interpreting them as a correction to some nonradiative process. For instance, hard photon emission will act as a severe background to the study of quarkonium transitions [3] and the search for excited leptons [4]; as another example the process $e^+e^- \to \gamma\nu\bar{\nu}$ may be used as a accurate way of counting the number of neutrino types, while the "lowest order" process $e^+e^- \to \nu\bar{\nu}$ is completely undetectable [5].

We will now describe the major qualitative features of radiative effects.

1. *Overall magnitude*

In a typical experimental situation a rough guess for Δ, the magnitude of the radiative correction, is in first order of perturbation theory given by

$$\Delta \sim \frac{2\alpha}{\pi} \ln \left(\frac{s}{m_e^2}\right) F_{corr} ,$$

(2.1)

9

where contributions of higher order in α have been neglected. Here $\alpha \sim 1/137$ is the fine structure constant, $s = 4E_b^2$ is the square of the centre-of-mass energy (E_b being the beam energy), and m_e is the electron mass. F_{corr} is a quantity which is typically of order unity, but in some special situations it may become much larger (positive or negative). If F_{corr} is not strongly dependent on s, then also Δ is a smooth function of s. Setting $F_{corr} \equiv 1$, we find that Δ varies between 8.5 % at $\sqrt{s} = 5\,GeV$ and 11.7 % at $\sqrt{s} = 150\,GeV$.

2. *Infrared divergencies*

It is well known that for small energy k of the emitted photon the bremsstrahlung cross section is proportional to 1/k. The resulting divergence in the cross section can be regularized by giving the photon an extremely small but finite mass λ: the infrared divergence will then be connected with terms in the cross section that go as $\ln \lambda$. These terms are cancelled in all orders of perturbation theory [2] by similar terms with opposite sign that come from the virtual photon corrections. This leads to the two following conclusions. In the first place, there is no physically meaningful way to separate the virtual and real photon corrections to a given process and any treatment will have to deal simultaneously with the two contributions that, however, describe different final states. Secondly, whereas the virtual photon corrections are independent of the detailed experimental situation, the real photon contribution diminishes as the allowed phase space for bremsstrahlung becomes smaller, for instance if the bremsstrahlung can be detected with greater precision. In that case the $O(\alpha)$ correction may become large and negative, and higher order corrections become important, leading to an exponentiated form for the corrected cross section.

3. *Collinear peaking behaviour*

Apart from those situations where the lowest order cross section has large peaks (if any), the multidifferential bremsstrahlung cross section will in addition show high and narrow peaks whenever the bremsstrahlung photon is emitted parallel to one of the incoming or outgoing charged particles. For any such particle the bremsstrahlung cross section contains a factor $[(p+k)^2 - m^2]^{-1}$, where p and k denote the four-momenta of charged particle and photon, respectively, and m is the mass of the charged particle, which is taken to be small compared to the particle energy p^0. Usually $(p+k)^2$ will be much larger than m^2. If $\vec{k}$ is (nearly) parallel to $\vec{p}$, however,

10

$(p+k)^2$ will also be or order m^2, leading to the forementioned peak in the cross section. For instance, if the bremsstrahlung is emitted by a 20 GeV $e^{\pm}$ beam, the cross section rises with a factor 5×10^7 when the angle between $\vec{k}$ and $\vec{p}$ goes from 10 degrees down to 0. That the collinear peaks and the infrared divergence from the last section are closely related can be understood by making the following observation. The cross section is a Lorentz-invariant quantity, and can be evaluated in any coordinate frame. The energy k^0 of the photon *in the rest frame of the charged particle* (i.e. the coordinate frame where $\vec{p}=0$) is given by

$$k^0_{\text{rest system}} = \frac{1}{2m} \left((p+k)^2 - m^2 \right) \ . \tag{1.2}$$

From the above we see that this quantity is of order m when $\vec{p}$ and $\vec{k}$ are parallel in the lab system, so that the photon becomes soft if m becomes small. For finite m the cross section will not display a singularity in this situation, but a peak will occur leading to terms with ln m in the integrated cross section, as can be seen in eq. (1.1).

3. Event generators

From the above it is clear that the magnitude of radiative effects depends strongly on the allowed kinematical configurations, and therefore a treatment of these effects has to include a careful analysis of the experimental situation [6]. Concerning this, three remarks are in order. In the first place, the set of experimental cuts on the allowed phase space is usually far too complicated to allow for a fully analytic calculation of the radiative effects, and usually one has to rely on numerical methods to obtain the radiative correction. Simplifying the boundary conditions that describe the cuts on phase space, in order to make an analytic treatment possible, usually introduces into the result an error equal to or greater than the inaccuracy of a numerical integration with precise cuts.

Secondly, there are many quantities and distributions of interest, each defined experimentally in a different way, and hence influenced by radiative effects in a different way.

In the last place, with the increasing complexity of the detection apparatus, it becomes also necessary to examine carefully how this apparatus reacts to a given collision process: this is usually done by constructing a computer simulation of the detector.

In view of the above considerations it appears that the optimal way of studying radiative effects in complicated experimental situations is not to derive analytic or numerical expressions for the quantities of interest, but rather to construct a computer simulation of the radiative process itself i.e. an event generator. This is defined as a numerical program resulting in a set of four-vectors (the momenta of the final-state particles) where the probability for a given configuration of four-vectors to occur is given by some theory (in our case, usually quantum electrodynamics). The advantages of this approach are clear: it is conceptually very simple, and flexible in the sense that a generated sample of *events*, i.e. sets of four-momenta, can be used to simulate every quantity or distribution that is experimentally defined. By counting the number of events that survive a given set of experimental cuts one obtains a Monte Carlo estimate of the cross section. Also the generated events can be used as input for a detector simulation.

The above holds not only for radiative processes but for most scattering processes of interest: indeed, event generators have been constructed for processes like jet fragmentation as well [7]. However, the fluctuating behaviour of bremsstrahlung cross sections requires a careful treatment both of the probability distributions of interest and of the numerical problems which may be encountered in generating these distributions.

References

1. F.M. Renard, "Basics of electron-positron collisions", (Editions Frontières, Gif-sur-Yvette, 1981).

   P. Duinker, lectures given at the 18th International School of Subnuclear Physics at Erice, Italy, 1980 (NIKHEF-H/81-05).

   B. Wiik, lectures given at the 1981 Summer School of Theoretical Physics at Les Houches, France.

2. F. Bloch and A. Nordsieck, Phys.Rev. 52 (1937) 54.
   D.R. Yennie, S.C. Frautschi, and H. Suura, Ann.Phys. 13 (1961) 379.

3. See e.g.
   R. Partridge et al., Phys.Rev.Lett. 45(1980) 1150.

   B. Wiik, talk given at the 1975 Int. Symp. on Lepton and Photon Interactions at High Energies at Stanford, U.S.A.

4. See e.g.

R. Hollebeek, talk given at the 1981 Int. Symp. on Lepton and Photon
Interactions at High Energies at Bonn, Germany.

J. Branson, ibidem.

5. L. Ma and J. Okada, Phys. Rev. Lett. $\underline{41}$ (1978) 287.
K.J.F. Gaemers, R. Gastmans and F.M. Renard, Phys. Rev. $\underline{D19}$ (1979) 160.
G. Barbiellini, B. Richter and J.L. Siegrist, Phys. Lett. $\underline{106B}$ (1981) 414.

6. K.J.F. Gaemers, Ph.D. thesis, Leiden, 1974.
F.A. Berends and R. Gastmans, in: Electromagnetic Interactions of Hadrons,
eds. A. Donnachie and G. Shaw, Plenum Publ. Corp., 1978.

7. P. Hoyer et al., Nucl. Phys. $\underline{B161}$ (1979) 349.
A. Ali et al., Phys. Lett. $\underline{93B}$ (1980) 155.
R.D. Field and R.P. Feynman, Nucl. Phys. $\underline{B136}$ (1978) 1.
B. Anderson et al., Z. Phys. $\underline{C3}$ (1980) 223; Nucl. Phys. $\underline{B135}$ (1978) 273.

CHAPTER III

REMARKS ON MONTE CARLO TECHNIQUES

1. Introduction

   Having argued in the previous chapter that radiative processes can be
adequately studied using event generators, we will now proceed to give a
brief overview of the field of random-variable techniques, which are also
known as Monte Carlo methods. We will keep in mind the specific application
of these methods.

   Therefore, we will not go into any mathematical detail. Moreover, we want
to illustrate the motivations behind our particular approach rather than give
an exhaustive review of all existing methods.

   This chapter is organized as follows. In section 2 we will formulate our
problem in terms of the generation of a multidimensional probability
distribution. In section 3 we will indicate several possible ways to solve
this problem. In the last section we will comment on some technical details
concerning generation of random numbers, numerical inversion, and numerical
stability.

   On all the points neglected or only hinted at in this chapter, many good
monographs and reviews exist, for which we refer to refs. [1].

2. Multidimensional probability distributions

   The problem under consideration can be formulated as follows: given an
N-dimensional space of variables $\vec{x}$ (denoting the set $x_1, x_2, \ldots, x_N$), and a
probability distribution $f(\vec{x})$, i.e. a nonnegative, real and integrable
function [*], construct an algorithm for obtaining a number of definite,
uncorrelated values for $\vec{x}$ such that the probability that the components x_i lie
in the interval between y_i and $y_i + dy_i$ is given by $f(\vec{y}) dy_1 \, dy_2 \, \ldots \, dy_N$.

   In case the integrals over successive variables are known (preferably as
analytic expressions, although also numerical integrals can in principle be
used), the problem reduces to a set of one-variable problems as follows: we

---

[*] We will only consider continuous distributions here. It is possible to
treat also discrete probability distributions in the same way, by interpreting
them as generalized (δ) functions of a continuous variable.

14

denote the set of successive integrals by

$$f_N(x_1,\ldots,x_N) = f(x_1,\ldots,x_N)$$

$$f_{N-1}(x_1,\ldots,x_{N-1}) = \int f_N(x_1,\ldots,x_{N-1},x_N)dx_N$$

$$f_{N-2}(x_1,\ldots,x_{N-2}) = \int f_{N-1}(x_1,\ldots,x_{N-2},x_{N-1})dx_{N-1}$$

up to

$$f_1(x_1) = \int f_2(x_1,x_2)dx_2 \quad , \tag{3.1}$$

where all integrals run over the allowed range for the corresponding variable. Now $f_1(x_1)$ is a one-dimensional probability distribution for x_1, with the use of which we generate a value for x_1. Keeping x_1 fixed at this value, $f_2(x_1,x_2)$ can be interpreted as a one-dimensional probability distribution for x_2. In this way we can successively generate $x_2,x_3,\ldots,x_N$. We should keep in mind, however, that the *form* of the distribution for x_k may depend in a complicated way on the obtained values for $x_1,\ldots,x_{k-1}$; only $f_1(x_1)$ is free of parameters in this sense. In the following we will assume that the integrals $f_1,f_2,\ldots,f_{N-1}$ are known, and concern ourselves with the one-variable problem only.

3. Simulation techniques

In this section a short description will be given of different methods to generate values of x according to a one-dimensional probability distribution f(x). We assume the existence of a *random number generator*, i.e. a source of completely uncorrelated and equidistributed numbers between 0 and 1. We will denote such numbers with the symbol η. To compare the different methods we introduce the concept of *efficiency* of an algorithm, defined as the average number of times a probability distribution (or its primitive) has to be evaluated in order to obtain one random value for the variable. If in a computer program this evaluation is the most time-consuming part of an algorithm (for instance, if the function is very complicated), the efficiency will be a direct measure of the speed of this program.

Before describing the different methods to generate probability distributions, we would like to mention a feature of probability distributions which is often useful, the *superposition property* : in order to generate x according to f(x), we may split f(x) into a sum of probability distributions $h_i(x)$ such that

15

$$f(x) = \sum_i h_i(x) \tag{3.2}$$

and generate an x value according to one of the h_i, where the integrals $\int h_i(x)dx$ are used as weights to determine the choice of h_i in a random way.

The two basic methods for generating x between x_0 and x_1 according to $f(x)$ are:

1. *Rejection algorithm* ("hit-or-miss" method)

For this method we have to know the maximum f_m of $f(x)$ in the interval $[x_0, x_1]$. A value x is then generated as follows:

(i)   Using the random number generator, pick two numbers η_1 and η_2 between 0 and 1.

(ii) Determine x and y as follows:

$$x = x_0 + (x_1 - x_0)\eta_1$$

$$y = \eta_2 f_m . \tag{3.3}$$

(iii) if $y > f(x)$ go back to (i);

if $y \le f(x)$ accept the obtained value for x.

In words: choose random points in the smallest rectangle in which the curve describing $f(x)$ fits, and drop all points that happen to lie above this curve.

It is immediately clear that the efficiency E will be:

$$E = \frac{1}{f_m(x_1 - x_0)} \int_{x_0}^{x_1} f(x)dx. \tag{3.4}$$

For smooth functions E can be of order 1; for sharply peaked functions, however, E can be close to zero. An advantage of this method is, that it can be trivially generalized to more dimensions, without needing the integrals $f_2, \ldots, f_{N-1}$.

2. *Inversion algorithm*

We define the cumulative distribution $F(x)$ as

$$F(x) = \int_{x_0}^{x} dx' f(x') . \tag{3.5}$$

Then the values for x can be generated by solving

$$F(x) = \eta F(x_1) \tag{3.6}$$

for random η between 0 and 1. By construction, this equation has one solution in the interval $[x_0, x_1]$. In words: the values of the cumulative distribution $F(x)$ are distributed uniformly if x is distributed according to $f(x)$.

The efficiency of this method is given by

$$E = \frac{1}{N} , \tag{3.7}$$

where N is the number of evaluations of $F(x)$ (or its inverse F^{-1}) necessary to solve eq. (2.5). There are two possibilities:

(i) F^{-1} is known analytically: in this case $E=1$ or $\frac{1}{2}$ (depending on whether we have to calculate $F(x_1)$ or not).

(ii) F^{-1} is not known analytically: we then have to rely on a numerical method in order to solve the equation. The simplest and most straightforward way to do this is by means of a binary search, using the following algorithm: divide the interval $[x_0, x_1]$ in two equal parts and determine in which part the root x of eq. (3.6) lies by evaluating $F\left(\frac{1}{2}(x_0+x_1)\right)$. By iterating this procedure we can determine the value of x with (in principle) arbitrary precision. The efficiency for such an algorithm is

$$E = \frac{\ln 2}{p \ln 10} \sim \frac{0.3}{p} , \tag{3.8}$$

where p is the desired number of significant decimals in x. More sophisticated methods than binary search may, of course, give a better efficiency for a given accuracy, but can also be more time-consuming.

If $F(x)$ is not known explicitly, the inversion algorithm can still be used by approximating $f(x)$ by a histogram and using the corresponding cumulative histogram as an approximation of $F(x)$; however the accuracy of this procedure is limited, and it certainly is unreasonably slow for secondary distributions as $f_2, \ldots, f_{N-1}$ where for every $\vec{x}$ a new series of cumulative histograms would have to be set up.

The essence of the second method is that it uses a transformation of the variable (from x to $F(x)$) such that the distribution becomes uniform. The more sophisticated methods we will describe now show an application of the same principle.

3. *Adaptive numerical algorithms* (stratified sampling)

These are used in programs that try to calculate multidimensional
integrals numerically by optimizing the choice of the integration points.
This is usually done by dividing the integration region into subvolumes,
and redividing or combining these subvolumes in such a way that every sub-
volume will give the same contribution to the total integral (this is
estimated by taking a few integration points inside each subvolume). This
process is iterated several times until the estimated error is below some
desired level. Ideally, by that time the integration points are
distributed according to the function to be integrated, and can be used as
generated values for $\vec{x}$. Several of such routines have been developed [2].
In principle these programs are suited for any probability distribution,
and their efficiency is approximately

$$E \gtrsim \frac{1}{N} , \tag{3.9}$$

where N is the number of iterations the program used to obtain the optimal
distribution of subvolumes. In practice, however, these programs are
usually less sensitive to peaks in the function that do not run parallel
to a coordinate axis, or that are such that they can not be singled out
by a simple coordinate transformation. Also, since usually the sub-
integrals are not all equal, even if sufficiently many iterations have
been taken to obtain the desired accuracy, the events are to be assigned
a weight which depends on the integral over the subvolume they are in, and
a rejection procedure as in 1) can then be used to obtain the events.
This inevitably means a loss of accuracy; also, usually the maximum weight
is either unknown or very large in comparison to the average weight.
The above indicates that an adaptive routine will usually be less accurate
as an event generator than when it is used for its original goal, namely
to calculate an integral. In the last case one would of course not have to
assign weights and reject part of the integration points.

4. *Importance sampling algorithm*

This method aims at combining the rejection and the inversion method
while keeping the advantages of both. One has to find an approximant $g(x)$
for the desired probability distribution $f(x)$ which satisfies the following
conditions:
a) $g(x)$ is also a probability distribution;
b) the approximation must be good, i.e. the ratio $f(x)/g(x)$ should not

18

fluctuate too wildly;

c) the cumulative distribution $G(x)$ of $g(x)$ can be inverted without too much trouble.

If $g(x)$ and $G(x)$ can be found under the above conditions, we can generate x as follows:

(i) generate x according to the distribution $g(x)$, using the inversion method.

(ii) assign to this value for x a weight $w(x)$, defined as

$$w(x) = \frac{f(x)}{g(x)} \, . \tag{3.10}$$

The rejection algorithm is now applied to reject or accept the obtained value for x, using $w(x)$ as a distribution. The maximum w_m of $w(x)$ which has to be known can either be determined empirically, or derived from $g(x)$ and $f(x)$: the latter may be difficult in case $g(x)$ and $f(x)$ are very complicated.

This approach can easily be extended to more dimensions, in which case the two following remarks are in order. In the first place, it is not necessary to use a rejection algorithm for each generated x_i; it is as efficient (and hence faster) to apply the rejection algorithm after having generated all components of $\vec{x}$. Secondly, it can be useful to perform a transformation of variables $x_1, x_2, \ldots, x_N \rightarrow y_1, y_2, \ldots, y_N$ before approximating $f(\vec{x})$; in that case, it is necessary to include the Jacobian $|\partial(x_1, x_2, \ldots, x_N)/\partial(y_1, y_2, \ldots, y_N)|$ into the definition of the weight function $w(\vec{x})$.

The efficiency of this method is of course the product of the efficiencies of both steps as given in eqs. (3.4,7). From this it follows that it is not wise to choose an approximation which is extremely simple but gives a bad weight distribution, or which is very good but takes a long time to be inverted. If $f(\vec{x})$ is sharply peaked, $g(\vec{x})$ should have all the peaks both at their correct place and with the right magnitude within a reasonable factor.

An advantage of the above approach is that it has much room for optimizing either the speed of the algorithm or its numerical stability: also peaking behaviour which is difficult in the sense mentioned in the last section can usually be treated; a drawback is, that it requires good understanding of the behaviour of $f(\vec{x})$, and that for every new case a new set of approximants, cumulative integrals and algorithms to generate the variables must be constructed.

Of course there exist more methods than the ones given above. We want to mention here the method of control variates and of antithetic variates. Since these approaches explicitly introduce correlations between the random variables (thus destroying their "randomness"), they are in our opinion less suited for the direct simulation of physical events.

Since the late 1940's (when the first serious work on Monte Carlo techniques started) there has developed a whole arsenal of ways to generate many distributions using clever, fast or elegant tricks that do not fall into any of the mentioned categories. Many of them can be found in refs. 7).

4. Some technical remarks

In this section we want to make several comments on more technical aspects of the described methods for numerical simulation.

1) *Random number generators*

We have assumed the existence of a source of truly random numbers. However, the most extensive set of such numbers contains 2500000 values [3] which may still be rather limited for our purposes. Normally one uses arithmetic algorithms which result in a completely determined sequence of numbers (i.e. not at all random), where the relation between subsequent numbers is such that *for most purposes* they appear to be uncorrelated. The most widely used random number generator of this type is the so-called multiplicative congruential generator [4] which both has reasonable "randomness" and is at the same time very simple: one multiplies a random number with a fixed constant and uses the least significant decimals of the result as the new random number [*]. It has been shown, however, that this type of algorithm suffers from one fundamental drawback: if the subsequent (pseudo-)random numbers are divided into successive n-tuples and these are interpreted as the coordinates of points in an n-dimensional unit hypercube, *all* points will lie on a very limited number of parallel planes in the cube [5]. This regular behaviour can of course give rise to unexpected correlations in the Monte Carlo results. For instance, in the

---

[*] The quality of randomness and equidistribution of the numbers yielded by this algorithm depend on the choice of the multiplier. There exist many different statistical tests that, however, may not be conclusive: for instance, none of these tests discovered the feature mentioned in the text.

case we will consider in the next chapter a 5-dimensional phase space has to
be generated: if every random number from the generator would be used to
give precisely one phase space variable, all generated events would lie
on only 220 planes or less in this phase space, which would be easily
visible in a large part of this phase space. This number holds for a
computer with a word length of 32 bits. If the points were truly randomly
distributed, this number could be of the order of 10^8, of which no effect
could be seen.
One way out of this problem would be to generate groups of numbers at the same
time, and shuffling their order. Another method is used in the following part
of this thesis where not all random numbers that are generated are trans-
formed into phase space variables, owing to several rejection procedures.
This ensures a certain effective shuffling of the random number sequence.

2) *Inversion*

As described before, the inversion method for generating distributions
is a mapping of a random number into a variable by the inverse of the
cumulative distribution. If the mapping is available as an analytical
expression, it can be evaluated with great precision; in case we have to
invert numerically, the accuracy will usually be less. In particular,
when the inversion is done by simple binary searching with n iterations,
the possible results of the mapping are "quantized" into 2^n discrete
equidistant values. This may lead to a situation where a peak in the
cross section is (owing to the favourable statistics) seen to fall apart
into a series of parallel peaks [6]. Use of either more iterations, or a
more sophisticated inversion (e.g. using interpolation) will improve on
such a situation.

3) *Choice of variables*

As stated before, the bremsstrahlung cross section is sharply peaked as
a function of the solid angles of the particle momenta. Due to this fact,
many events will occur for which the cosine of such an angle (which is the
phase-space variable, rather than the angle itself) lies very close to +1
or -1. For instance, the distribution of the angle θ of the photon with
respect to one of the beam axes will show peaks near $\cos \theta = 1$ and $\cos \theta = -1$,
with 50% of the events having $1 - |\cos \theta| < 3 \times 10^{-5}$, and 10% of the events
having $1 - |\cos \theta| < 5 \times 10^{-9}$ (for $E_b = 15 \text{GeV}$). In such situations much
numerical accuracy may be lost in the calculation due to the fact that we
have a limited number of decimals available in a floating-point

representation. The numerical stability of the generation of such
sharply peaking distributions can be considerably improved by taking for
the variable to be generated not $|\cos \theta|$ but $1 - |\cos \theta|$ which will be a
number close to zero and can be represented with a small exponent in
floating-point notation.

References

1. See F. James, Rep.Prog.Phys. 43 (1980) 1145, and the references quoted
   there.
   T.M. Hammersley and D.C. Handscomb, Monte Carlo Methods, Methuen, London,
   1964.
   B. Jansson, Random Number Generators, Petterson, Stockholm, 1966.

2. Some adaptive routines:
   RIWIAD, by
   B. Lautrup, Proc. 2nd Colloquium on advanced computing methods in
   theoretical physics, Marseille (1971) I-58;
   DIVONNE2, by
   J. Friedman, SLAC Computation Research Group Technical Memo CGTM 188,
   1977;
   VEGAS, by
   G.P. Lepage, Journ. Comput. Phys. 27 (1978) 192.

3. N.A. Frigerio and N.A. Clark, Trans. Am. Nucl. Soc. 22 (1975) 283;
   Argonne Report ANL/BS-26-4 (1978).

4. This algorithm was first proposed by D.H. Lehmer, Ann. Comp. Lab. Harvard
   Univ. 26 (1951) 141.

5. G. Marsaglia, Proc. Nat. Acad. Sci 61 (1968) 25.

6. T. Bork and H. Burkhardt, private communication.

7. C.J. Everett and E.D. Cashwell: A Monte Carlo sampler (Los Alamos
   Scientific Laboratory Informal Report ANL/ES-26, 1972).

CHAPTER IV

PAIR PRODUCTION OF MUONS AND QUARKS

1. Introduction

In the last two chapters it was argued that radiative processes can conveniently be studied by using event generators, and the general methods involved in Monte Carlo simulations were described. In this chapter, these results will be applied to the processes of muon pair production and quark pair production. There are several reasons for choosing these as an illustration. In the first place, they are subject to intensive study. Many of the important parameters of QCD, such as the strong coupling constant, the number of quark colours and species, and the spin of the gluon are extracted from quark production, and muon (or tau lepton) production is one of the cleanest and most straightforward ways to obtain information on the neutral current sector of the electroweak interactions. In the second place, both processes are described by exactly the same Feynman diagrams in the lower orders of perturbation theory, and can therefore be treated the same way (indeed, even gluon bremsstrahlung can be described in this way, at least up to first order). Finally, they have all characteristic features of bremsstrahlung processes mentioned in chapter II. Of course there are many other e^+e^- scattering processes of great physical interest, like Bhabha scattering ($e^+e^- \rightarrow e^+e^-$), photon pair production ($e^+e^- \rightarrow \gamma\gamma$), and the so-called two-photon processes ($e^+e^- \rightarrow e^+e^-\mu^+\mu^-$, etc.). However, on the one hand these processes have cross sections very different from muon production, which would necessitate a different set of formulae, and on the other hand no essentially new results on the technique of generating events would be obtained. Therefore we do not deal with them here, but refer to the literature.

The method which will be used to simulate the processes under consideration will be that of importance sampling described in section 3 of the last chapter. To do this, we need the following ingredients:

1. exact expressions for the cross section in all parts of phase space;
2. useful approximants to these exact, but generally complicated formulae;
3. a set of algorithms to generate events according to the approximations used;
4. a way of assigning weights to each generated event.

23

The rest of this chapter, in which we will discuss the first of these points, is organized as follows: in section 2 the lowest order cross section is given, and it is shown how to describe either muon or quark production by changing the relevant parameters. In sections 3, 4 and 5 we treat the virtual corrections, and the contributions from soft and hard bremsstrahlung, respectively.

Finally, some technical remarks are in order. In the first place we will throughout the following chapters assume that we are in the ultrarelativistic limit, i.e. the masses of all fermions are assumed to be small·as compared to their energies. However, masses are kept wherever their absence would cause divergencies. For muons, this is completely justified at PETRA/PEP energies already (m_μ = 106 MeV, as compared to the typical energy E_b = 18000 MeV). The values of the light quark masses are rather uncertain (estimates ranging from several to several hundred MeV), but are in any case small. The masses of the heavier particles (tau lepton, m_τ = 1782 MeV, charm and bottom quarks, $m_c \sim$ 1500 MeV, $m_b \sim$ 4500 MeV) are not really negligible, but their major effect can be taken into account rather easily without a real change in the results. In the second place, the expressions for the cross sections are usually lengthy. Since we are interested in the structure of the formulae rather than in their details, many of them have been listed in appendix A, while in the text we concentrate only on those features which are relevant to the Monte Carlo techniques. In the last place, wherever the word 'muon' appears, the statement holds equally well for quarks.

2. Lowest order cross section

In this section the expressions for the pair production cross sections for muons and quarks are given. As stated above these differ only in the values of the occurring coupling constants and masses. In order to make a systematic treatment possible we have normalized all weak coupling constants to the electromagnetic charge of the relevant antiparticle and those charges to that of the positron, so that this charge occurs as an overall factor everywhere. The values of the couplings to the photon and the Z_0 boson are arbitrary as far as our treatment is concerned. Below we present a table of their values in the simplest model for the electroweak interactions, the $SU(2) \times U(1)$ model of Glashow, Weinberg and Salam (1) with only one Higgs doublet.

In this table, $x = 4 \sin^2\theta_w$, and $y = 4 \sin\theta_w\cos\theta_w$, where θ_w is the weak mixing angle. In principle, also the pair production of neutrinos can be described with the following formulae, resulting in the process mentioned in

Table 1. Coupling constants in the standard model

fermion type	electric charge Q	weak vector coupling v	weak axial vector coupling a
e, μ, τ	$+1$	$(x-1)/y$	$-1/y$
$u, c(,t)$	$-2/3$	$(x-3/2)/y$	$-(3/2)/y$
d, s, b	$+1/3$	$(x-3)/y$	$-3/y$

chapter II.

The remaining parameters of the neutral weak current, namely the mass and width of the Z_0 boson, are also in principle free. In the standard model mentioned above they are given by

$$M_z = \left[\frac{\pi\alpha}{G_F\sqrt{2}}\right]^{\frac{1}{2}} \frac{4}{y} \sim \frac{149.2 \text{ GeV}}{y} \quad , \quad G_F = 1.165 \times 10^{-5} \text{ GeV}^{-2}$$

$$\Gamma_z = \frac{\alpha M_z}{3y^2}\left[N_\ell\left(1 + (1-x)^2\right) + 3N_u\left(1 + (1-\frac{2}{3}x)^2\right) + 3N_d\left(1 + (1-\frac{1}{3}x)^2\right) + 2N_\nu\right],$$

$$(4.1)$$

where N_ℓ, N_u, N_d, N_ν are the number of types of leptons, up-quarks, down-quarks and neutrinos, respectively, in which the Z_0 can decay. At present, good guesses are

$$M_z \sim 88.6 \text{ GeV} , \quad \Gamma_z \sim 2.5 \text{ GeV} , \tag{4.2}$$

corresponding to a value for $\sin^2\theta_w$ of about 0.23.

By suitable changes in the masses and couplings, also the hadronic resonances J/ψ and T can be described by the formulae given in the following; however, the width of these resonances is typically much smaller, and consequently the radiative corrections are usually such that higher orders in perturbation theory than the first have to be included in the treatment which is not done here.

The lowest order matrix element is given by the two diagrams of fig. 1, which represent the exchange of either a photon or a Z_0 boson in the s-channel. In terms of spinors and propagators, we have

$$M_0 = \frac{ie^2 QQ'}{s} \left[\bar{v}(p_+)\gamma^\mu u(p_-) \cdot \bar{u}(q_-)\gamma_\mu v(q_+) + \right.$$

$$\left. \chi(s)\bar{v}(p_+)(v+a\gamma^5)\gamma^\mu u(p_-) \cdot \bar{u}(q_-)(v'+a'\gamma^5)\gamma_\mu v(q_+) \right]$$

$$\chi(s) = \frac{s}{s-M_z^2+iM_z\Gamma_z} \quad . \tag{4.3}$$

Here p_+ (p_-) is the four-momentum of the incoming positron (electron), q_+ (q_-) is the momentum of the outgoing antimuon (muon), and $s = (p_+ + p_-)^2$ is the total invariant mass square of the system. Quantities with prime are connected with the outgoing particles, and those without one relate to the initial state. It is useful to define the following currents:

$$V^\mu = \bar{v}(p_+)\gamma^\mu u(p_-) \qquad V'^\mu = \bar{u}(q_-)\gamma^\mu v(q_+)$$

$$A^\mu = \bar{v}(p_+)\gamma^5\gamma^\mu u(p_-) \qquad A'^\mu = \bar{u}(q_-)\gamma^5\gamma^\mu v(q_+) \quad . \tag{4.4}$$

If we do not consider particle polarization (i.e., we average over the spins of the e^+ and e^- and sum over the spins of the $\mu^+\mu^-$) the following relations hold:

$$|V\cdot V'|^2 = |V\cdot A'|^2 = |A\cdot V'|^2 = |A\cdot A'|^2 = s^2(1+\cos^2\theta)$$

$$(V\cdot V')(A\cdot A')^* = (V\cdot A')(A\cdot V')^* = 2s^2\cos\theta$$

$$(V\cdot V')(V\cdot A')^* = (V\cdot V')(A\cdot V')^* = (V\cdot A')(A\cdot A')^* = (A\cdot V')(A\cdot A')^* = 0 \quad , \tag{4.5}$$

where we have defined θ as the polar angle of the positive muon with respect to the e^+ beam axis. If later on the effect of beam polarization is taken into account, these products are the only quantities that are modified. We have normalized the spinors such that $\bar{u}(p)u(p) = 2m$.

The differential cross section is given by

$$\frac{d\sigma_0}{d\Omega} = \frac{\alpha^2 Q^2 Q'^2}{4s^3} \left| (V\cdot V') + \chi(s)\big((vV+aA)\cdot(v'V'+a'A')\big) \right|^2$$

$$= \frac{\alpha^2 Q^2 Q'^2}{8s} \left[A(s)(1-\cos\theta)^2 + B(s)(1+\cos\theta)^2 \right]$$

$$d\Omega = d\phi d\cos\theta$$

$$A(s) = 1 + 2(vv'-aa')\mathrm{Re}\,\chi(s) + \big((v^2+a^2)(v'^2+a'^2) - 4vv'aa'\big)|\chi(s)|^2$$

$$B(s) = 1 + 2(vv'+aa')\mathrm{Re}\,\chi(s) + \big((v^2+a^2)(v'^2+a'^2) + 4vv'aa'\big)|\chi(s)|^2 \ , \tag{4.6}$$

where ϕ is the trivial azimuthal angle of the μ^+ around the beam, and the

total cross section as a function of s is defined as

$$\sigma_0(s) = \frac{2\pi\alpha^2 Q^2 Q'^2}{3s} \left[A(s) + B(s) \right] .$$ (4.7)

In the case of quark pair production we of course have to multiply all cross sections with 3, accounting for the existence of three colour types of every quark flavour.

3. Virtual corrections

The first of the higher-order contributions to muon pair production that should be included are the virtual corrections, described by the set of all Feynman diagrams that have the same initial and final state as the lowest order process, and contain one closed loop. The complete set , consisting of some 90 diagrams [*] in the standard model referred to in the previous section, has been calculated in the literature (2). In this thesis we will, however, restrict ourselves to a subset of 22 diagrams, namely those containing an extra virtual photon, and the self-energy diagram of the virtual photon that is exchanged in lowest order. There are several reasons for this. In the first place, a complete calculation is clearly model dependent and may therefore not be useful if for instance a comparison between different weak interaction models is to be made. In the second place, the virtual corrections, since they describe also a two-particle final state, only have the effect of changing the angular dependence of the lowest-order cross section (and, of course, the total cross section). It turns out that this modification results in an angular dependence which is a very complicated function, but nevertheless very smooth. Including the total weak effect does not change this. Also, for those regions where the complete weak corrections have been calculated (that is, not close to the Z_0 pole), their total magnitude turns out to be rather small, and the QED corrections dominate (3). In the last place, the set of corrections that are described below form a gauge-invariant set and give a correction which is model-independent.

The various contributions have appeared many times in the literature (4), and we will list them without any derivation. The precise expressions can be found in appendix A.

---

[*] The exact number of diagrams is, of course, dependent on the gauge used which determines the absence or presence of diagrams with ghosts.
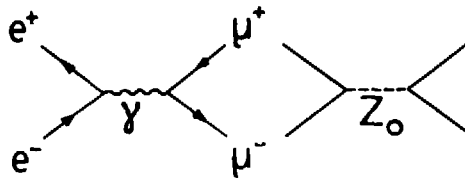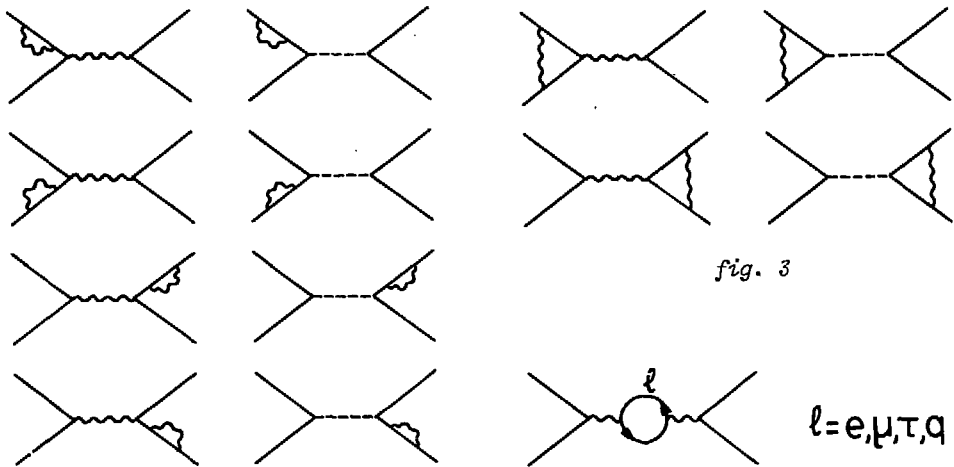
fig. 1

fig. 2

fig. 3
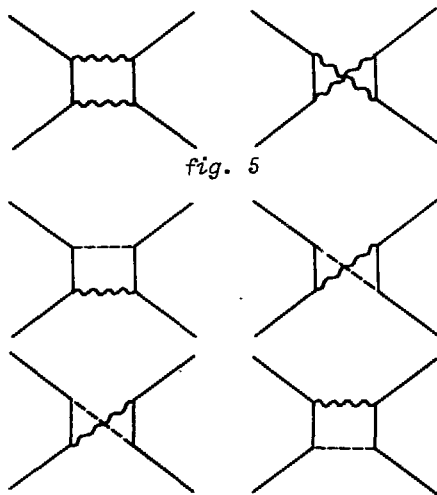

$\ell = e, \mu, \tau, q$
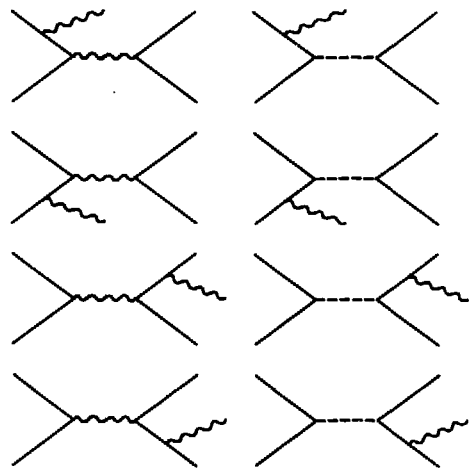
fig. 4

fig. 5

fig. 6

fig. 7

1) *Self energy diagrams (fig. 2)*

In our case these contributions vanish after renormalization since the particles are on mass shell.

2) *Vertex corrections (fig. 3)*

These are proportional to the lowest-order vertex, and can be written as a scalar function multiplying the lowest-order matrix element:

$$M_{vc} = e^2 M_0 \left[Q^2 F(s,m_e^2) + Q'^2 F(s,m_\mu^2) \right] . \tag{4.8}$$

The function $F(s,m^2)$ is infrared divergent after renormalization, and can be regularized by giving the photon a small but finite mass λ.

3) *Vacuum polarization diagrams (fig. 4)*

These describe the self-energy of the electromagnetic field due to virtual fermion loops, resulting in a change in the photon propagator of Eq. (4.3):

$$M_{vp} = - \frac{ie^2 QQ'}{s} (V \cdot V') \Pi(s) . \tag{4.9}$$

The vacuum polarization $\Pi(s)$ can be split up according to the different fermions that contribute:

$$\Pi(s) = \Pi_e(s) + \Pi_\mu(s) + \Pi_\tau(s) + \Pi_h(s) . \tag{4.10}$$

Here the lepton contributions are known exactly because their masses are known. The hadronic contribution $\Pi_h(s)$ ('quark loops') can be calculated by the following dispersion relations:

$$\mathrm{Re} \; \Pi_h(s) = \frac{s}{4\pi^2\alpha} \; \mathcal{P} \int_0^\infty \frac{\sigma_h(s')}{s'-s} \, ds' ,$$

$$\mathrm{Im} \; \Pi_h(s) = \frac{s}{4\pi\alpha} \, \sigma_h(s) , \tag{4.11}$$

where $\mathcal{P}$ denotes the principal value definition of the integral. These relate the vacuum polarization to $\sigma_h(s)$, the total cross section for hadron production. This is probably the most accurate method of determining $\Pi_h(s)$ because of the uncertainties due to the quark masses and the effects of confinement at these 'low' energies. Indeed, the above relations can be used to estimate the masses of the lighter quarks. The integral (4.11) can be numerically evaluated to a precision of about 0.5 %, the main uncertainty coming from the

experimental data on the low-energy region (up to a value of E_b of a few GeV)(5).

4.1) *Box diagrams with 2 photons (fig. 5)*

Their contribution, which is ultraviolet finite but infrared divergent, can be written as follows:

$$M_{\gamma\gamma} = \frac{ie^4 Q^2 Q'^2}{s} \left[(V_1 + 2i\pi V_2)(V \cdot V') + (A_1 + 2i\pi A_2)(A \cdot A') \right] , \qquad (4.12)$$

where V_1, V_2, A_1, A_2 are given in appendix A. It is these diagrams that are (with the corresponding bremsstrahlung terms) responsible for the main change in angular dependence, and give a forward-backward asymmetry which at lower energies suppresses the effect of the weak interactions on the asymmetry.

4.2) *Box diagrams with one Z_0 and one photon (fig. 6)*

For simplicity, we have kept from these only the part proportional to the Z_0 propagator. This part contains the infrared divergence, and has moreover been calculated for the (slightly simpler) case of J/ψ exchange. The contribution to the matrix element reads:

$$M_{z\gamma} = \frac{ie^4 Q^2 Q'^2}{s} \chi(s) \left((vV + aA) \cdot (v'V' + a'A') \right) \delta_{z\gamma} . \qquad (4.13)$$

where again $\delta_{z\gamma}$ is given in the appendix A.

Adding up all these corrections, we obtain for the virtual correction to the matrix element:

$$M_v = M_{vc} + M_{vp} + M_{\gamma\gamma} + M_{z\gamma} \qquad (4.14)$$

and the contribution to the differential cross section reads

$$\frac{d\sigma_v}{d\Omega} = \frac{d\sigma_0}{d\Omega} + \frac{1}{32\pi^2 s} \, \text{Re} \, M_0 M_v^* , \qquad (4.15)$$

which can be evaluated easily, using eq. (4.5).

Before turning to the bremsstrahlung contributions, we want to make a few remarks. In the first place, the above expression is still (infrared) divergent, which forces us to take bremsstrahlung into account. Secondly, the angular dependence is smooth, except for the very forward and backward regions, where sharp peaks occur due to the box diagrams. Since these peaks are only logarithmic (and hence integrable) they can still be interpreted as probability distributions. In the last place, the total event rate is of course altered by the above corrections. Carrying out an integration over Ω

30

is, however, not very easy and not even necessary, as we will see in the next chapter.

4. Soft bremsstrahlung

Apart from the virtual corrections it is, as we have seen, necessary to include bremsstrahlung contributions as well, in order to cancel the infrared divergences. The physical reason behind this mathematical argument is, that since the photon is massless, always some amount of energy may be radiated off in any experiment with finite resolution [*]. It is therefore natural to divide the bremsstrahlung contribution into two parts, one from those photons that go undetected in any experiment (i.e. their energy, and their effect on the kinematics of the remaining particles is within experimental resolution), and the other part containing those photons that can in principle be seen. In this section we treat the first of these parts.

It is rather easy to obtain the matrix element for soft bremsstrahlung in a very good approximation. This is done in two steps. By dropping the photon four-momentum k wherever it appears in the numerator of the eight brems- strahlung diagrams of fig. 7, it can easily be shown that the bremsstrahlung matrix element is that of the lowest order, multiplied with an overall factor containing the photon momentum and polarization. Some care has to be taken, however, that the correct dependence of the Z_0 propagator is kept, since a small energy loss due to bremsstrahlung may cause a large change in this propagator close to its peak (this effect is of course very important for extremely narrow resonances like the J/ψ or T, but even for the relatively wide Z_0 resonance it cannot be neglected). In this way we can write for the matrix element:

$$M_s = -\frac{ie^3 QQ'}{s}\left[(V \cdot V')(QF_p - Q'F_q) + \left((vV+aA)\cdot(v'V'+a'A')\right)\left(Q\chi(s')F_p - Q'\chi(s)F_q\right)\right]$$

$$F_p = \frac{p_- \cdot \varepsilon}{p_- \cdot k} - \frac{p_+ \cdot \varepsilon}{p_+ \cdot k} , \qquad F_q = \frac{q_- \cdot \varepsilon}{q_- \cdot k} - \frac{q_+ \cdot \varepsilon}{q_+ \cdot k} , \qquad (4.16)$$

where $s' = s(1 - k^0/E_b)$ is the energy in the Z_0 propagator after bremsstrahlung

---

[*] For an electron in an external field admitting bound states with finite energy differences, the energy can in principle be measured with zero error. In that case the infrared problem is probably absent (7).

radiation, and k^μ, ε^μ are the photon momentum and polarization vector, respectively. The photon polarization is, as is usual, assumed to be un-detected. The second step consists of taking the square of the matrix element (4.16) and integrating it over the soft photon phase space, i.e. over all solid angles and over energies up to some value E_0. The energy integral can be split into two parts again. The first is the region up to some extremely small value E_s, where the factorization holds with s'=s. In this region, we again give the photon a small mass λ. The second region is between E_s and E_0, and here we have to take the dynamical effect of the Z_0 propagator into account, but the photon can be taken massless. The final result is given by

$$\frac{d\sigma_s}{d\Omega} = \frac{\alpha^2 Q^2 Q'^2}{8s} \left[\tilde{A}(s)(1-\cos\theta)^2 + \tilde{B}(s)(1+\cos\theta)^2 \right] \, ,$$

$$\tilde{A}(s) = \delta_s^Q + 2(vv'-aa')\mathrm{Re}\,\chi(s)\delta_s^I + \left((v^2+a^2)(v'^2+a'^2) - 4vv'aa' \right)|\chi(s)|^2\delta_s^R \, ,$$

$$\tilde{B}(s) = \delta_s^Q + 2(vv'+aa')\mathrm{Re}\,\chi(s)\delta_s^I + \left((v^2+a^2)(v'^2+a'^2) + 4vv'aa' \right)|\chi(s)|^2\delta_s^R \, ,$$

$$(4.17)$$

where again the occurring quantities are further defined in appendix A.

Adding the virtual and soft bremsstrahlung contributions we obtain the corrected cross section for those final states that simulate the elastic ($\mu^+\mu^-$) case. The cross sections are plotted in figs. 8 a,b,c for three different energies. As can be seen, the angular distribution is rather smooth, and the total event rate is down from the lowest order by a considerable amount if E_0 is small. Again, these results are similar to those for the narrow hadronic resonances, with one difference: in the last case, the resonance width is typically much smaller than E_0, and therefore the resonance falls either completely inside or completely outside the soft photon region. In the case of the Z_0, however, this is not true any more and a careful treatment of the 'tail effect' of the resonance is necessary (3,6).

Finally we want to comment on the inclusion of higher orders into the correction. If no hard bremsstrahlung is taken into account, the correction is clearly rather large and negative. The higher-order contributions from soft bremsstrahlung can be estimated, for instance by using a coherent-state formalism as in ref. (6). However, if we include the (positive) contribution from hard bremsstrahlung, the total correction usually becomes rather modest, removing the a priori need for a higher-order calculation. At values of s equal to, or slightly less than, M the hard bremsstrahlung is virtually absent, but for those energies the (still uncalculated) weak corrections are

Figs. 8

Differential cross section for muon pair production in the soft region. $d\sigma/d\Omega$ is set out along the vertical axis against $\cos\theta$ along the horizontal axis. The cross sections are given in nanobarn. The various parameters have the following values:

$M_z = 88.6$ GeV, $\Gamma_z = 2.5$ GeV, $Q = Q' = 1$, $v = v' = -0.0475$,

$a = a' = -0.594$, $E_0 = 0.01\ E_b$.

The solid line is the cross section for the lowest order (i.e. corresponding to the diagrams of fig. 1 only), while the dashed line is the cross section with the virtual and soft bremsstrahlung corrections.

It can be seen that the angular dependence of both cross sections is very similar, except for very large values of $|\cos\theta|$. This justifies the approximation in eq. (5).
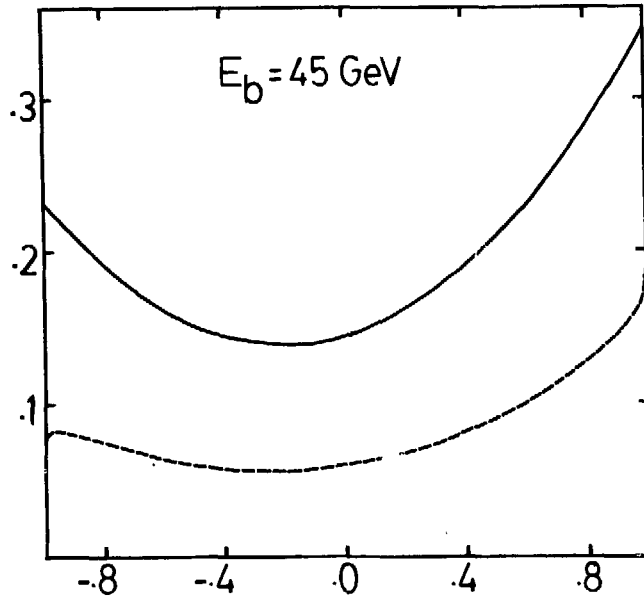
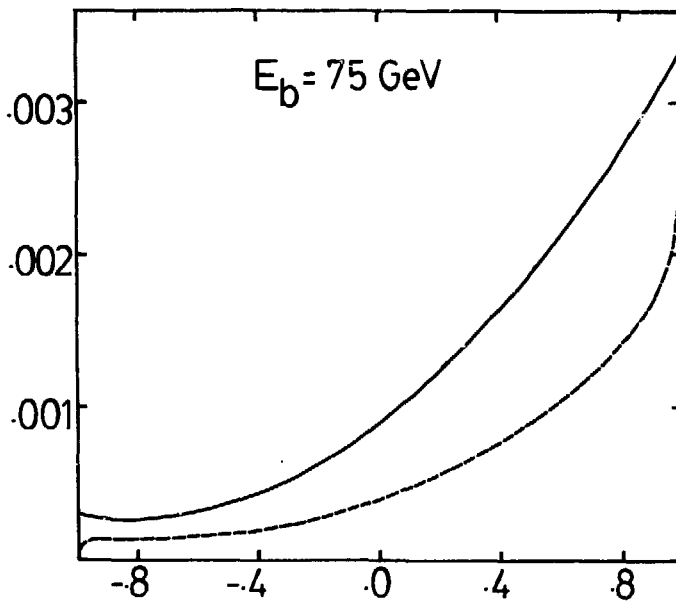

fig. 8a

$E_b = 45$ GeV

fig. 8b

$E_b = 75$ GeV

fig. 8c

34
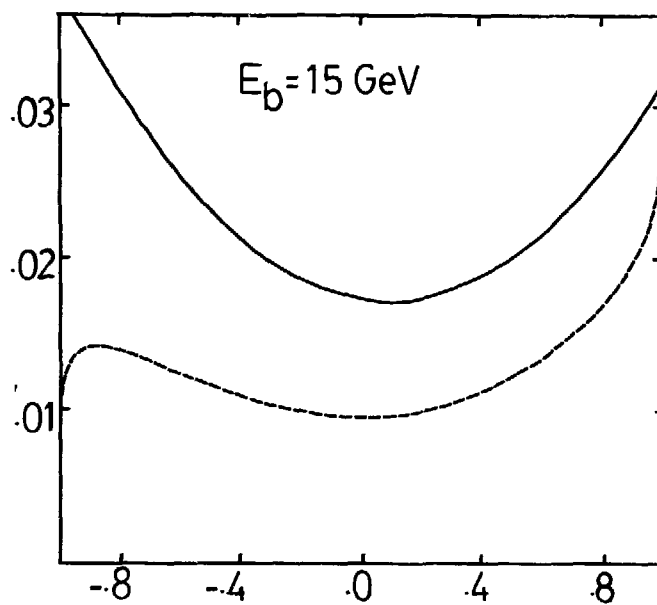
presumably larger than the higher-order QED corrections. In all, we see no urgent need for including these corrections at the present stage of theory and experiment.

5. Hard bremsstrahlung

In this last section we present the hard photon cross section, which is given by the same diagrams (fig. 7) that also describe the soft photon emission. Because now the energy and direction of the photon are measurable quantities, the five-dimensional phase space cannot easily be reduced to a two-dimensional one by integrating over the photon momentum, as was the case for soft bremsstrahlung. Also, the choice of variables is more complicated because the contributions to the hard photon cross section are not easily given in one set of independent variables only. Since we are in any case not very interested in analytical expressions for the various distributions (in view of the remarks in section 3 of chapter II) we will postpone the choice of variables until the next chapter, and concern ourselves here only with the amplitude squared, summed and averaged over spins as before, which we call the cross section for this moment.

The calculation of bremsstrahlung cross sections is rather complicated. In the first place, there are usually several diagrams that contribute (in our case 8, giving rise to 36 products to be evaluated). Because each diagram has a different denominator, which is connected to the propagator of the radiating particle, it is by no means straightforward to combine the different contributions into a reasonable form. Moreover, in most cases there are many invariant products of four-momenta in the problem, and it is not a priori clear which set of them is best to express the cross section in. Indeed, it has turned out (8) that choosing a 'minimal' set of independent invariants does not give the simplest expression for the cross section for most single-bremsstrahlung processes that have been considered. Some time ago it was discovered that the bremsstrahlung cross sections can be written in a simple and elegant form, very similar to the soft photon cross section (9). Recently, a formalism has been developed (10) which leads in a natural way to these simple forms by calculating the amplitude rather than its square, thus avoiding the necessity of combining many terms, and doing so for the various helicities of the fermions and the photon (using a special gauge).

The cross section for $e^+e^- \to \mu^+\mu^-\gamma$ can be written as follows in terms of invariants (3):

$$|M_B|^2 = 4e^6 Q^2 Q'^2 \left\{ Q^2 \left[\frac{1}{4s'\kappa_+\kappa_-} \left(A(s')(t^2+t'^2) + B(s')(u^2+u'^2) \right) \right. \right.$$

$$\left. - \frac{m_e^2}{2s'^2\kappa_-^2} \left(A(s')t^2 + B(s')u^2 \right) - \frac{m_e^2}{2s'^2\kappa_+^2} \left(A(s')t'^2 + B(s')u'^2 \right) \right]$$

$$+ Q'^2 \left[\frac{1}{4s\kappa_+'\kappa_-'} \left(A(s)(t^2+t'^2) + B(s)(u^2+u'^2) \right) \right.$$

$$\left. - \frac{m_\mu^2}{2s^2\kappa_-'^2} \left(A(s)t^2 + B(s)u'^2 \right) - \frac{m_\mu^2}{2s^2\kappa_+'^2} \left(A(s)t'^2 + B(s)u^2 \right) \right]$$

$$+ QQ' \frac{1}{4ss'} \left(\frac{u}{\kappa_+\kappa_-'} + \frac{u'}{\kappa_-\kappa_+'} - \frac{t}{\kappa_+\kappa_+'} - \frac{t'}{\kappa_-\kappa_-'} \right) \left(C(s,s')(t^2+t'^2) + D(s,s')(u^2+u'^2) \right)$$

$$\left. + QQ' \frac{(s-s')M_z\Gamma_z}{2\kappa_+\kappa_-\kappa_+'\kappa_-'} \varepsilon_{\mu\nu\rho\sigma} p_+^\mu p_-^\nu q_+^\rho q_-^\sigma \left(E(s,s')(t^2-t'^2) - F(s,s')(u^2-u'^2) \right) \right\} ,$$

$$s = (p_+ + p_-)^2 \qquad t = (p_+ - q_+)^2 \qquad u = (p_+ - q_-)^2 \qquad \kappa_\pm = p_\pm \cdot k$$

$$s' = (q_+ + q_-)^2 \qquad t' = (p_- - q_-)^2 \qquad u' = (p_- - q_+)^2 \qquad \kappa_\pm' = q_\pm \cdot k$$

$$C(s,s') = 1 + (vv'-aa')\mathrm{Re}\left(\chi(s) + \chi(s') \right) + \left((v^2+a^2)(v'^2+a'^2) - 4vv'aa' \right) \mathrm{Re}\left(\chi(s)\chi(s')^* \right)$$

$$D(s,s') = 1 + (vv'+aa')\mathrm{Re}\left(\chi(s) + \chi(s') \right) + \left((v^2+a^2)(v'^2+a'^2) + 4vv'aa' \right) \mathrm{Re}\left(\chi(s)\chi(s')^* \right)$$

$$E(s,s') = \frac{1}{2ss'} (va'-v'a) \left(\frac{1}{s'} |\chi(s')|^2 - \frac{1}{s} |\chi(s)|^2 \right) +$$

$$+ \frac{s-s'}{s^2s'^2} \left((v^2+a^2)v'a' - (v'^2+a'^2)va \right) |\chi(s)|^2 |\chi(s')|^2$$

$$F(s,s') = \frac{1}{2ss'} (va'+v'a) \left(\frac{1}{s'} |\chi(s')|^2 - \frac{1}{s} |\chi(s)|^2 \right)$$

$$+ \frac{s-s'}{s^2s'^2} \left((v^2+a^2) v'a' + (v'^2+a'^2)va \right) |\chi(s)|^2 |\chi(s')|^2 , \tag{4.18}$$

where $\varepsilon_{\mu\nu\rho\sigma}$ is the completely antisymmetric tensor, with $\varepsilon_{0123} = +1$.

Here the various contributions can be easily recognized. The cross section splits naturally into initial state radiation, final state radiation, and the interference between the two. The term with $\varepsilon_{\mu\nu\rho\sigma}$ originates because of the difference in complex phase between $\chi(s)$ and $\chi(s')$. Since it has an overall factor Γ_z and also vanishes in case any two particles are collinear, its effect is very small. The effect of nonzero mass of the fermions can be seen in the

36

occurrence of terms with m_e^2, m_μ^2 which can, even in the ultrarelativistic limit, not be neglected because of the double poles in the propagators.

References

1. S. Glashow, Nucl.Phys. 22 (1961) 579.
    S. Weinberg, Phys.Rev.Lett. 19 (1967) 1264.
    A. Salam, in: Elementary Particle Physics, ed. H. Svartholm (Almquist and Wiksells, Stockholm).

2. G. Passarino and M. Veltman, Nucl.Phys. B160 (1979) 151.

3. F.A. Berends, R. Kleiss, and S. Jadach, Leiden preprint (1981) (to appear in Nucl.Phys. B).

4. See, e.g. F.A. Berends and R. Gastmans, in: Electromagnetic Interactions of Hadrons, ed. A. Donnachie and G. Shaw (Plenum, 1978), and the references quoted therein.

5. N. Cabibbo and R. Gatto, Phys.Rev. 124 (1961) 1577.
    F.A. Berends and G. Komen, Phys.Lett. 63B (1976) 432.
    H. Burkhardt, private communication.

6. V. Chung, Phys.Rev. B140 (1965) 1110.
    M. Greco and G. Rossi, Nuovo Cim. 50 (1967) 168.
    N. Papanicolaou, Phys.Rep. 24 (1976) 229.
    M. Greco, G. Pancheri-Srivastava, and Y. Srivastava, Nucl.Phys. B101 (1975) 234; Nucl.Phys. B171 (1980) 118.

7. R. Gastmans, private communication.

8. F.A. Berends, R. Kleiss, P. de Causmaecker, R. Gastmans, and T.T. Wu, Phys.Lett. 103B (1981) 124.

9. F.A. Berends, R. Gastmans, and T.T. Wu, paper submitted to the 1979 International Symposium on Lepton and Hadron Interactions at High Energies, Fermi Lab.

10. P. de Causmaecker, R. Gastmans, W. Troost, and T.T. Wu, DESY preprint 81-050 (to appear in Nucl.Phys. B).
    F.A. Berends, R. Kleiss, P. de Causmaecker, R. Gastmans, W. Troost, and T.T. Wu, Leuven preprint KUL-TF-81/8 (to appear in Nucl.Phys. B).

CHAPTER V

APPROXIMANTS AND EVENT GENERATION

1. Introduction

    In the last chapter the first of the necessary ingredients to construct a
simulation program was given, namely the set of exact formulae. In this
chapter we will indicate how these exact expressions can be approximated in
order to allow for fast and accurate event generation, and describe possible
algorithms for doing so.   It is clear that the specific method developed here
is not the only possible one. However, in practice all event generators for
processes like the one under consideration that make use of importance sampling
will run more or less along the lines sketched in the following.

    As a first step it is necessary to deal with the infrared problem.   The
conceptual difficulty arising here is that we have to connect two cross
sections describing different final states, of which only the sum has a
physical meaning.   We can solve this by dividing the bremsstrahlung phase
space into two parts.   The first part, where the photon energy is below a
certain value E_0, will be called the *soft* part.   The second (*hard*) part
contains those events that have a photon energy between E_0 and the maximum
desired energy E_{max}.   If E_0 is small enough photons from the soft part will in
practice be undetectable, because their effect on the kinematics of the final
state (acollinearity etc.) is negligible.   To the total cross section in the
soft part is added the lowest-order cross section and the virtual corrections
to it.   The first step in the generation of any event will be the choice of
one of the two parts, using the (approximate) total cross sections of both as
relative weights for this choice.   If an event is chosen to lie in the soft
region, the photon energy is assumed to be zero, the event has elastic
kinematics and the angular distribution is given by the soft cross section.
In the other case, the event is generated according to the hard bremsstrahlung
cross section (cf. eq. (4.18)).   From this we see that E_0 is restricted by
two conditions:

1) E_0 must be so small that it is a good approximation to neglect the photon
    momentum in the cross section and in the kinematics;

2) E_0 must be so large that the soft cross section (both total and
    differential) is positive everywhere.

Usually a value of $E_0 = 0.01\ E_b$ satisfies both restrictions. As an illustration, this corresponds to a maximum acollinearity angle of the muon tracks of $0.5°$. Another approach would be to use an exponentiated form for the cross section, where the dominant parts of higher order corrections are taken into account by rewriting the cross section as follows:

$$\sigma(k^0 < E_0) = \sigma_0\left(1 + \beta\ \ln\left(\frac{E_0}{E_b}\right) + F(E_0)\right) \to \sigma_0\left(1 + F(E_0)\right)\left(\frac{E_0}{E_b}\right)^\beta . \qquad (5.1)$$

Here β is a constant and $F(E_0)$ is finite for vanishing E_0. In this way an explicit division of phase space is avoided, since the cross section vanishes if E_0 goes to zero (1). However, such an exponentiation is only really justified for infinitesimally small E_0, and it is therefore practically impossible to incorporate measurable photon momenta into such a method without biasing the generated events sample in some (complicated) way.

We now turn to the hard part. As will be seen in the next chapter, the bremsstrahlung cross section is usually dominated by the initial-state and final-state radiation, while the interference between the two is a minor effect, and we drop it from eq. (4.18) as a first step in the approximation. Furthermore, it is seen that the initial state radiation peaks if the angle between the photon and e^+ or e^- momenta is small, while the final state radiation has its peak for small angles between the photon and μ^+ or μ^-. Therefore the two contributions are most easily described (and generated) in terms of different sets of variables. To this end we use the superposition property: if an event is generated in the hard part of phase space, it will be distributed according to one of the two cross sections. Again this is determined using the two approximate total cross sections as relative weights.

We have now split the cross section into three pieces: soft part, initial state radiation and final state radiation. For each of the three we must construct an approximant, its successive integrals and total approximate cross section, and a generation algorithm. For the respective pieces this is done in the next three sections. The weights (which have to be assigned to the events in order to obtain the exact distribution) are given in the next chapter.

2. <u>Soft part</u>

In order to simulate the soft cross section it is necessary to know the

total event rate in the soft part of phase space. The differential cross section in this part is known as a one-dimensional distribution (if we do not consider the trivial azimuthal angular dependence) but this is a complicated expression. It is of course possible to calculate its integral either analytically or numerically, but it is easier to realize that a Monte Carlo simulation is equivalent to an integration, and the exact soft cross section is in fact calculated during the generation of events. It is therefore enough to use some estimate of the total soft cross section. The approximate character of this procedure can be corrected for by a suitable factor in the definition of the event weights. The final distribution will then be correct no matter what the estimate was, but the efficiency will of course depend on it. One method to obtain such an estimate is to keep from the virtual and soft bremsstrahlung corrections only the dominant (and preferably angle-independent) terms. The estimated total cross section can then easily be calculated. For instance, only the vertex corrections and the corresponding soft bremsstrahlung, and the vacuum polarization are taken into account. Another method is to numerically estimate the total cross section by evaluating the differential cross section for a few values of $\cos\theta$. The approximant becomes

$$\frac{d\sigma^{app}}{d\Omega} = \frac{3\sigma^{est}}{16\pi\left(A(s)+B(s)\right)} \left(A(s)(1-\cos\theta)^2 + B(s)(1+\cos\theta)^2\right) , \qquad (5.2)$$

and the total cross section is

$$\sigma^{app} = \sigma^{est} , \qquad (5.3)$$

where σ^{est} is the estimated soft total cross section, and $A(s)$, $B(s)$ are given in eq. (4.6).

The generation of $\cos\theta$ for a soft event is most easily done by using the superposition property in order to generate either $(1-\cos\theta)^2$ or $(1+\cos\theta)^2$ with relative probabilities $A(s)$ and $B(s)$. The distribution $(1+x)^2$ can be generated using analytic inversion:

$$x = 2\eta^{1/3} - 1 , \qquad (5.4)$$

where η is a random number equidistributed between 0 and 1, as in chapter II. Since the approximant is a rather smooth function, we could of course also use rejection to generate $\cos\theta$. The efficiency of such an algorithm will in this case always lie between 1/3 and 2/3 so inversion is slightly better here. The azimuthal angle is of course just a random number between 0 and 2π.

3. Initial state radiation

In this section we will give a treatment of the initial state radiation which can also be applied to other processes in which the final state is formed by exchange of one particle (photon, Z_0 boson, etc.). Since in such processes the part of the Feynman diagrams corresponding to the formation of the final state is unchanged if bremsstrahlung is emitted from the intial state, it is logical to assume that the bremsstrahlung cross section is connected in some simple and process-independent way to that for the non-radiative process. This was first shown in ref. 2 for the total cross section in the case of photon exchange. Later it was generalized to the case of multidifferential cross sections (3) and more general neutral currents (4). The connection between the lowest order and bremsstrahlung cross sections is the following: let the lowest order cross section be given as follows:

$$\frac{d\sigma_0}{d\vec{q}_1 \dots d\vec{q}_N} = f(s, \vec{e}; \vec{q}_1, \dots, \vec{q}_N) , \qquad (5.5)$$

where $\vec{q}_1, \dots, \vec{q}_N$ are the momenta of the final state, evaluated in their centre-of-mass frame, and $\vec{e}$ is the unit vector in the direction of $\vec{p}_+ - \vec{p}_-$. Then the cross section for bremsstrahlung from the initial state is given by

$$\frac{d\sigma_I}{d\vec{q}_1 \dots d\vec{q}_N dk^0 d\Omega_\gamma} = \frac{\alpha k^0 Q^2}{4\pi^2 s} \left[g_+(k) f(s', \vec{e}_+; \vec{q}_1, \dots, \vec{q}_N) + \right. $$
$$\left. + g_-(k) f(s', \vec{e}_-; \vec{q}_1, \dots, \vec{q}_N) \right]$$

$$g_\pm(k) = \frac{(s' + 2\kappa_\mp)^2}{2\kappa_+ \kappa_-} - \frac{m_e^2 s'}{\kappa_\mp^2} , \qquad (5.6)$$

where again $\vec{q}_1, \dots, \vec{q}_N$ are evaluated in their centre-of-mass frame, k^μ in the lab frame, and $\vec{e}_+$ ($\vec{e}_-$) are the unit vectors in the direction of $\vec{p}_+ - \vec{p}_- + \vec{k}$ ($\vec{p}_+ - \vec{p}_- - \vec{k}$). This can, of course, be explicitly verified in eq. (4.18). Upon integration over all momenta $\vec{q}_1, \dots, \vec{q}_N$ we obtain for the photon momentum distribution

$$\frac{d\sigma_I}{dk^0 d\Omega_\gamma} = \frac{\alpha k^0 Q^2}{4\pi^2 s} \cdot \left(g_+(k) + g_-(k) \right) \sigma_0(s') , \qquad (5.7)$$

and for the photon spectrum

$$\frac{d\sigma_I}{dk^0} = \frac{\alpha Q^2}{\pi} \left(\ln \frac{s}{m_e^2} - 1 \right) \frac{1 + (s'/s)^2}{k^0} \sigma_0(s') . \qquad (5.8)$$

The last two formulae are identical to the results in ref. 2.

The above formulae provide us directly with a way to generate the initial state radiation part, in four steps.

1) Generate the photon energy according to eq. (5.8). Due to the resonant structure of $\sigma_0(s)$ in our case, this function may be quite involved. There is a peak for small values of k^0, which is just the onset of the infrared divergence. For values of s above M_z^2, there will also be a peak for those values of k^0 for which $s' = s(1-k^0/E_b)$ is close to M_z^2. Near the resonance, both peaks coincide, and the photon spectrum falls off very rapidly. Although possible, it is neither easy nor elegant to approximate the spectrum by a form that covers all these possibilities. A better approach is to calculate analytically the cumulative spectrum (which is given in appendix B) and invert it numerically. This inversion can be speeded up considerably by applying the following argument. During numerical inversion, the cumulative spectrum is evaluated many times. The results can be stored in a table, so that in the course of generating an event sample the inversion can gradually be replaced by a search through this table, which can be made very fast. This is of course only possible because the photon spectrum is free of parameters in the sense of section 3 of chapter III. One could also, of course, at the beginning of a generation run tabulate the cumulative spectrum by using some adaptive one-dimensional routine (in one dimension, ordinary quadrature is usually more accurate than Monte Carlo quadrature). Both methods give us, as a side result, also the exact value for the total cross section for initial state radiation.

2) Generate the photon solid angle. In the absence of polarization we again have to worry only about the polar angle, which is distributed according to eq. (5.7). We can approximate this distribution by

$$\frac{d\sigma_I}{dk^0 dz d\phi} \sim \frac{\alpha Q^2}{4\pi^2} \frac{1+(s'/s)^2}{k^0} \sigma_0(s') \left[\frac{1}{e+z} + \frac{1}{e-z}\right]$$

$$z = \cos < (\vec{p}_+, \vec{k}) \; , \qquad e = 1 + 2m_e^2/s \; , \tag{5.9}$$

and generate either $(e-z)^{-1}$ or $(e+z)^{-1}$ with equal probability. The distribution $(e-x)^{-1}$ is generated analytically by

$$x = e - (e-1) \left(\frac{e+1}{e-1}\right)^\eta \; . \tag{5.10}$$

To the generated value of z we now assign the following weight:

$$w = \left[s^2 + s'^2 - 8\kappa_+\kappa_- - \frac{2m_e^2 s'\kappa_+}{\kappa_-} - \frac{2m_e^2 s'\kappa_-}{\kappa_+} \right] \bigg/ \left[s^2 + s'^2 \right] \qquad (5.11)$$

and we decide to keep the z value or to try again, depending on this
weight using the rejection algorithm. Also we decide which of the two
axes $\vec{e}_+$ or $\vec{e}_-$ we will choose to generate the muon momenta. The
probability of choosing $\vec{e}_+$ is given by the relative magnitude
$g_+/(g_++g_-)$.

We want to remark here that $g_+(k)$ or $g_-(k)$ can actually become negative
when $1-|z|$ becomes very small. In that case it is no longer possible
to use them as probabilities. However, for such values of z the two
orientation axes $\vec{e}_+$ and $\vec{e}_-$ coincide so it is unimportant which one we
choose. We therefore leave out the mass terms (proportional to m_e^2) in
$g_+/(g_++g_-)$, so that the probability for orienting the event towards $\vec{e}_+$
is

$$\frac{g_+(k)}{g_+(k)+g_-(k)} \sim \frac{(2E_b - k^0 + k^0 z)^2}{2\left[(2E_b - k^0)^2 + k^0{}^2 z^2 \right]} \ . \qquad (5.12)$$

By taking for the azimuthal angle a random number in $[0,2\pi]$ we can then
construct the photon four-momentum, and the muon c.m. frame.

3) Generate the muon momenta in their c.m. frame, taking some arbitrary
   axis for the beam direction. The muon solid angle is distributed
   according to

$$\frac{d\sigma_0(s')}{d\Omega} \propto A(s')(1-\cos\theta)^2 + B(s')(1+\cos\theta)^2 \ , \qquad (5.13)$$

   and can be generated in the same way as in the soft part. It is
   interesting to notice that the absence of beam polarization makes not
   one azimuthal angle trivial, but two, as can be seen above.

4) Construct the four-momenta of the muons in the lab frame. To this end
   we rotate the 'beam axis' of the last step to either $\vec{e}_+$ or $\vec{e}_-$, depending
   on the choice made, and then boost the resulting vectors back to the
   lab frame.

The generation method outlined in this section is also applicable to other
processes where the final state (without the bremsstrahlung photon) is formed
in the decay of one vector or axial vector particle (4). Moreover it is exact
if we restrict ourselves to purely initial state radiation. Since in the
process under consideration also radiation from other particles is taken into

account, we will nevertheless have to weigh also the events from this part.

4. Final state radiation

From eq. (4.18) it is seen that the cross section for final state radiation can be obtained from that for initial state radiation by making the substitution $p_+, p_- \leftrightarrow -q_+, -q_-$. It is difficult, however, to make use of this property to treat the final state radiation with a formalism similar to that in section 3 since of course p_+ and p_- are always fixed, while q_+ and q_- are unknown at first. Also, such a treatment would only be appropriate for this particular process, so that no general formalism for final state radiation would result anyway. Instead we shall use a more 'standard' approach.

As a first step in the approximation the mass terms (proportional to m_μ^2) are dropped in the final state radiation part of eq. (4.18). By putting them into the weight function they will be accounted for in the final result. Secondly the symmetry of the cross section under the interchange $p_+, q_+ \leftrightarrow p_-, q_-$ is used to retain only the terms proportional to t^2 and u'^2 in the numerator, with an extra overall factor of 2. When an event has been generated, we will in one-half of the cases put $\vec{q}_+ \leftrightarrow -\vec{q}_-$, $\vec{k} \to -\vec{k}$ in the event, thus removing this bias. With these two approximations the cross section is written as follows:

$$d^5\sigma_F = \frac{4\alpha^3}{\pi^2 s} Q^2 Q'^4 \left(A(s)(1-\cos\theta)^2 + B(s)(1+\cos\theta)^2 \right) \frac{q_+^{0^2}}{2\kappa'_+\kappa'_-} \, d\Gamma \quad , \qquad (5.14)$$

where the five-dimensional phase space element $d\Gamma$ is given by

$$d\Gamma = d^4q_+ d^4q_- d^4k\,\delta(q_+^2)\delta(q_-^2)\delta(k^2)\theta(q_+^0)\theta(q_-^0)\theta(k^0)\delta^4(p_+ + p_- - q_+ - q_- - k)$$

$$= d\Gamma_1 d\cos\theta\, d\phi d\phi_\gamma$$

$$d\Gamma_1 = \frac{1}{8} dk^0 dq_+^0 = \frac{q_+^{0^2}k^0}{4s'} dk^0 dc_\gamma \quad ; \quad q_+^0 = \frac{1}{2} s'(2E_b - k^0 + k^0 c_\gamma)^{-1}$$

$$c_\gamma = \cos\!<(\vec{k}, \vec{q}_+) \quad . \qquad (5.15)$$

Here ϕ and ϕ_γ are the azimuthal angle of $\vec{q}_+$ around the e^+ beam, and of the photon around $\vec{q}_+$, respectively. The two alternative forms for $d\Gamma_1$ are both used in the following. The expression for q_+^0 in terms of k^0 and c_γ assumes the particles to be massless. It is described elsewhere (5) how justified this assumption is.

As is seen from eq. (5.14), the two azimuthal angles are in fact trivial random numbers in $[0,2\pi]$, while $\cos\theta$ again obeys the lowest-order distribution. It is generated in the same way as before. Upon integration over these three variables, we obtain

$$d^2\sigma_F = \frac{64\alpha^3}{3s} Q^2 Q'^4 \big(A(s) + B(s)\big) \; \frac{q_+^{0\,2}}{\kappa'_+ \kappa'_-} \; d\Gamma_1 = \frac{32\alpha Q'^2}{\pi} \sigma_0(s) \; \frac{q_+^{0\,2}}{\kappa'_+ \kappa'_-} \; d\Gamma_1 \; . \quad (5.16)$$

For the invariants κ'_+ and κ'_- two alternative expressions exist, that are both exact up to order $O(m_\mu^4/E_b^4)$:

$$\kappa'_+ = 2E_b(q_+^0 + k^0 - E_b + k^0 m_\mu^2/s') \; , \qquad \kappa'_- = 2E_b(E_b - q_+^0 + k^0 m_\mu^2/s') \; , \quad (5.17)$$

and

$$\kappa'_+ = k^0 q_+^0 (e^+ - c_\gamma) \; , \qquad \kappa'_- = k^0 q_+^0 \frac{s}{s'} (e^- + c_\gamma)$$

$$e^+ = 1 + 2m_\mu^2 s/s'^2 \; , \qquad e^- = 1 + 2m_\mu^2/s \; . \quad (5.18)$$

The first set allows for easy integration of the approximant, while the second set is slightly better for purposes of variable generation. Using eq. (5.17), we find for the photon spectrum

$$\frac{d\sigma_F}{dk^0} = \frac{\alpha}{\pi} Q'^2 \sigma_0(s) \left(\ln\!\left(\frac{s'}{m_\mu^2}\right) \frac{1 + (s'/s)^2}{k^0} - \frac{4k^0}{s} \right) \quad (5.19)$$

It is not difficult to derive the cumulative spectrum from this: it is given in appendix B. However, it is unnecessary for the generation of k^0, because the spectrum has none of the complicated resonant properties for the initial state radiation spectrum of eq. (5.8). We can use the approximation that the spectrum is described by $1/k^0$, and generate k^0 by the following algorithm and weight function:

$$k^0 = E_0 \left(\frac{E_{max}}{E_0}\right)^\eta \; , \qquad w = \frac{\ln\!\left(\frac{s'}{m_\mu^2}\right)\big(1 + (s'/s)^2\big) - 4k^{0\,2}/s}{2\ln\!\left(\frac{s}{m_\mu^2}\right)} \quad (5.20)$$

with very reasonable efficiency. E_{max} is again the maximum desired value for the photon energy, as given in section 1.

After having generated k^0 we now know both e^+ and e^- in eq. (5.18). The generation of c_γ is as follows: first the distribution

$$\frac{d\Gamma_1}{\kappa'_+\kappa'_-} = \frac{1}{8sk^0}\left(\frac{1}{e^+-c_\gamma} + \frac{1}{e^-+c_\gamma}\right)dk^0 dc_\gamma \tag{5.21}$$

is obtained by generating either $(e^+-c_\gamma)^{-1}$ or $(e^-+c_\gamma)^{-1}$ with relative probabilities given by

$$\ln\left(\frac{e^++1}{e^+-1}\right) \quad \text{and} \quad \ln\left(\frac{e^-+1}{e^--1}\right) \tag{5.22}$$

respectively. By assigning the generated value for c_γ a weight

$$w = (q^0_+/E_b)^2 \tag{5.23}$$

we can finally obtain the distribution (5.16).

Before concluding this section we want to make the following remark. In the above treatment of final state radiation it is clearly essential that the fermion (muon or quark) is massive in order to avoid all kinds of singularities. Since the quark masses are unknown (and often assumed to be zero for the lighter quarks) this could pose a problem. However, it is known (6) that for quantities that are sufficiently inclusive, all mass singularities (in our case, logarithms with m^2_μ in the argument) cancel against those of the virtual corrections. Therefore, any experimentally defined quantity that is not sensitive to the quark mass can be accurately simulated by the above methode, when a (smallish) quark mass is introduced as a cutoff. On the other hand, for a quantity that is sensitive to the quark mass, the simulation of massive distributions is of course indispensible, in order to obtain a fit to the quark mass. For these reasons we see no problem in the necessity of keeping a finite mass. Finally, in the case of very massive particles, for which $O(m^2_\mu/E^2_b)$ cannot be totally neglected, the final state radiation spectrum will not be changed very much, since it has no appreciable contribution from the higher k^0 values where the mass becomes important. The effect on the initial state radiation can of course be taken into account trivially by making the appropriate changes in $\sigma_0(s)$.

As stated in the introduction to this chapter, an event is chosen to lie in one of the three parts mentioned. The relative probabilities for this are the total (approximate) cross sections from these three regions. For the soft part, this is the quantity σ^{est}. For the initial state radiation, the corresponding cross section is the integrated form of eq. (5.8), while that for the final state radiation is given by the integral over the spectrum (5.19).

References

1. F. Bloch and A. Nordsieck, Phys. Rev. $\underline{52}$ (1937) 54.
2. G. Bonneau and F. Martin, Nucl. Phys. $\underline{B27}$ (1971) 381.
3. F.A. Berends and R. Kleiss, Nucl. Phys. $\underline{B178}$ (1981) 141.
4. F.A. Berends and R. Kleiss, Leiden preprint (to be published).
5. F.A. Berends and R. Kleiss, Nucl. Phys. $\underline{B177}$ (1981) 237.
6. T. Kinoshita, J. Math. Phys. $\underline{3}$ (1962) 650.
   T.D. Lee and M. Nauenberg, Phys.Rev. $\underline{B133}$ (1964) 1549.

CHAPTER VI

EVENT WEIGHTS

1. <u>Introduction</u>

In this chapter the last part of our event generation method will be
discussed, namely the weighing procedure. If a generated event has been
assigned a weight, it can be used in two ways. The first possibility is to
keep the event together with its weight in the further analysis. Then use is
made of every generated event, but events with extremely small or large
weights may cause loss of efficiency or large fluctuations in the result,
respectively. It is therefore desirable to have a reasonable weight
distribution. The second approach is to use the rejection method on the
weight, as indicated in chapter III. The accepted events are then
"unweighted", resulting in a more realistic event sample than in the first
case, which may be nice e.g. for purposes of studying the behaviour of
detection apparatus. However, since events are rejected, this method is
always less efficient than the first one. In the following, we will denote
by *trial events* those events that have been generated and to which a weight is
assigned, but which have not yet passed a rejection algorithm.

In studying the results of an importance-sampling event generator, the
weights of the trial events can be considered as stochastic variables. The
weight distribution $n(w)dw$ is defined as the number of trial events that have
weight in the interval $[w,w+dw]$. Its first two moments are the total number of
trial events N and their total weight W, respectively:

$$N = \int_0^{w_m} dw\, n(w)$$

$$W = \int_0^{w_m} dw\, w\, n(w) \; . \tag{6.1}$$

Here w_m is the largest occurring weight, an important parameter. In the ideal
case where no approximations have to be made to generate events, the weight
distribution is just a δ function around 1:

$$n(w) = N\delta(w-1) \; . \tag{6.2}$$

The number of trial events N_{acc} that survive the rejection procedure is given by

$$N_{acc} = W/w_m \cdot \tag{6.3}$$

From this we see that it is important to have w_m not too large, and W/N not too small, in order to obtain reasonable efficiency of the whole event generator.

As mentioned before, the approximate cross sections for the given process are assumed to be known. From these and the weight distribution, the exact cross section can be obtained by

$$\sigma_{exact} = \frac{W}{N} \, \sigma_{approx} \tag{6.4}$$

Since the weight distribution is known only after a sample of trial events has been generated, we can also obtain it by comparing the number of trial events with the number of accepted events:

$$\sigma_{exact} = \frac{N_{acc}}{N} \, w_m \, \sigma_{approx} \tag{6.5}$$

2. Technical remarks

Before deriving the expressions for the weights in the three cases we have considered, the following remarks are in order. In the first place, formally the cross section $d\sigma$ corresponding to a given event contains the infinitesimal phase space element $d\Gamma$. Since we may use different expressions for the phase space in the different cases of soft part, initial state radiation and final state radiation, the correct weight may not be just the ratio of the appropriate squared matrix elements, but could also contain a Jacobian, as mentioned in chapter III. In the second place, one should be careful to take the various exact and approximate expressions into account only in those parts of phase space in which they are defined. In the present process this is not a problem but situations may arise (as in Bhabha scattering) where the hard bremsstrahlung phase space has to be split up in many overlapping regions. In the third place sometimes functions have been generated for which the integral was known exactly buy which were generated using a small approximation-rejection loop, as was done for instance in eqs.(5.11, 20, 23). Those weights have already been taken into account and should, of course, not be included again in the trial event weight. In the last place, the technique of

importance sampling allows one to make approximations not only in the exact formulae with which one started, but also in the intermediate integration steps. The corresponding weights should then also be included. As an illustration, consider the two-dimensional distributions $g(x,y)$ given by:

$$g(x,y) = \frac{f(y)}{x+\epsilon_0+\epsilon(y)} \qquad 0 \leq x \leq 1 \; , \tag{6.6}$$

where $f(y)$ is some function which is easy to generate, and both $\epsilon(y)$ and ϵ_0 are very small. The value for x can be generated as in eq. (5.10), and the distribution for y is then given by

$$\int_0^1 dx\, g(x,y) = f(y)\, \ln\left[\frac{1+\epsilon_0+\epsilon(y)}{\epsilon_0+\epsilon(y)}\right] \; . \tag{6.7}$$

This distribution may be hard to generate if $\epsilon(y)$ is not simple. However, we can generate y according to

$$f(y)\, \ln\left[\frac{1+\epsilon_0}{\epsilon_0}\right] \quad , \tag{6.8}$$

and assign to the trial a weight defined as

$$w = \ln\left[\frac{1+\epsilon_0+\epsilon(y)}{\epsilon_0+\epsilon(y)}\right] \Big/ \ln\left[\frac{1+\epsilon_0}{\epsilon_0}\right] \; . \tag{6.9}$$

Notice that we could also have aproximated $g(x,y)$ by

$$g(x,y) \rightarrow \frac{f(y)}{x+\epsilon_0} \tag{6.10}$$

But then the weight would have to be defined as

$$w = \frac{x+\epsilon_0}{x+\epsilon_0+\epsilon(y)} \tag{6.11}$$

which may fluctuate much more than the previous expression. This approach is typically very useful when the peaking value of one variable is expressed in terms of the other variables as a function which is not varying very much but makes the integral, such as eq. (6.7), hard to handle.

3. Soft part

The weight of a soft event is derived rather easily, since there is only

one approximant to the cross section in this case, and the exact and
approximate expressions have the same phase space variables, so that no
Jacobian is necessary. The weight is given by

$$w_{soft} = \frac{d^2\sigma_v + d^2\sigma_s}{d^2\sigma_{app}} \quad , \tag{6.12}$$

where $d^2\sigma_v$, $d^2\sigma_s$ are the lowest order cross section plus virtual corrections
and the soft bremsstrahlung cross section, given by eqs. (4.15) and (4.17),
respectively. $d^2\sigma_{app}$ is the approximate form given in eq. (5.2). Since the
total number of trial events in the soft region was proportional to σ^{est}, it is
seen that this quantity will cancel exactly in the resulting cross section. One
remark is in order here. The approximate cross section does not, in our case,
exhibit the forward and backward singularities from the $\gamma\gamma$ boxdiagrams of eq.
(4.12). Therefore, the soft event weight is strictly speaking not bounded or
positive definite. However, the singularities are logarithmic and hence not
very strong, so that not many events will be produced at very large values of
$|\cos\theta|$. Also, muon pairs are usually not detected at very forward or backward
angles (typically, $|\cos\theta| < 0.98$) so that a slight distortion of the event
sample due to these out-of-range event weights has no effect. For other
processes (Bhabha scattering etc.) where small-angle scattering is very
important, more care may be necessary.

4. Hard part

In this section the weights of hard bremsstrahlung events will be derived.
From eq. (4.18) it is seen easily what are the approximate cross sections that
were used to generate the events. In the first place, the initial state
radiation part is given by the first two lines of eq. (4.18). In the final
state radiation we neglected the mass terms (line 4) and kept only the terms
in line 3. The two last lines were left out altogether. Since we used the
same phase space variables for both initial state and final state radiation,
the possible expressions for the Jacobians cancel in exact and approximate
cross section. Referring to the lines in eq. (4.18), the event weight is
given by

$$w_{hard} = 1 + \frac{X_4 + X_5 + X_6}{X_1 + X_2 + X_3} \quad , \tag{6.13}$$

where X_i denotes the terms on line i. Notice that the various overall factors can be left out. Again, we want to make several remarks. In the first place, the two separate contributions to the approximate cross section have been taken together here. This is necessary: the weight of an event is linear as far as the exact cross section is concerned (i.e. the superposition property holds), but it is not linear with respect to the approximate cross section (since it appears in the denominator of the expression). Using either one of the two approximants, but not both, would give wrong results. In the second place, in the various cross sections no integration has been performed, so that all peaks and cancellations are present (without being softened by integration over some peaking variables). Hence one should be careful to ensure the numerical stability of the expressions (cf. our remark at the end of chapter III). This is especially necessary if very hard photons are taken into account. In such situations the expression for $q_\pm^0$ in terms of the photon energy and the various angles may not be a good approximation, resulting in imperfect cancellations between terms (the weight may even become negative). One way out of this is to use the exact expression. Another possibility is to give the particle momenta a mass by performing the following transformation:

$$q_\pm^0 \to q_\pm^{0\,\prime} = \left[q_\pm^{0\,2} + m_\mu^2\right]^{\frac{1}{2}}$$

$$p_\pm^0 \to p_\pm^{0\,\prime} = \tfrac{1}{2}(q_+^{0\,\prime} + q_-^{0\,\prime} - k^0)$$

$$\vec{p}_\pm \to \vec{p}_\pm{}' = \vec{p}_\pm\left[p_\pm^{0\,\prime\,2} - m_e^2\right]^{\frac{1}{2}} / |\vec{p}_\pm| . \tag{6.14}$$

This transformation preserves all scattering angles but slightly modifies the particle energies. It corresponds to an effective shift in E_b of the order of m_μ^2/E_b^2, which is acceptable if this mass is not too large. After calculating the weight, the inverse transformation can then be applied. The third, and probably best, method is to perform possible cancellations by hand, by writing the cancelling quantities in variables which cancel explicitly, also in a computer program with finite numerical accuracy.

5. The weight distribution: a posteriori justification

As an illustration of the above, we present in this section a weight distribution, obtained by generating 10000 trial events in the manner described in the last three chapters (fig. 9). As can be seen, the weights are distributed in a way not very dissimilar to the ideal δ distribution. It should

also be noted that most of the higher and lower weight values belong to trial events from the soft region. The hard photon events are very peaked near w=1, while their weight is never larger than the theoretical bound of 2 (cf. the remarks in ref. 3 of chapter IV).

We want to stress at this point that it is only by inspection of distributions such as this one, that one can judge the efficiency and quality of an event generating procedure. It is not essential to have a strong peak around w=1, but the maximum weight should not be too much larger than the mean weight. In case no maximum weight can be given, but the distribution has an appreciable tail, it is almost sure that some doubtful approximation or numerical operation has been performed. A large number of events around w=0 poses no essential problem, but will diminish the efficiency. Negative weights should be avoided by all means, since they do not admit a statistical interpretation.
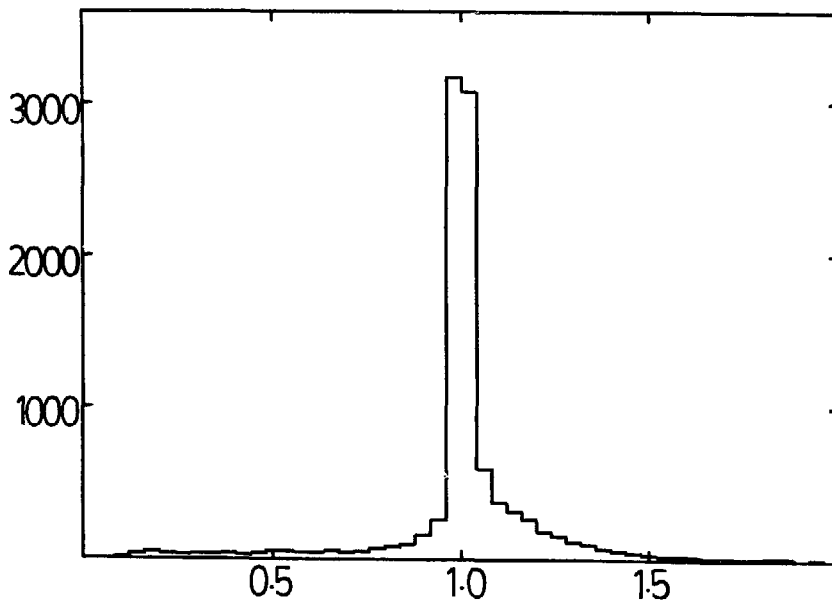
fig. 9. *Histogram of n(w). The event weights are distributed over 50 bins between 0 and 2. In this event sample, only two trial events fall outside this range.*

CHAPTER VII

POLARIZATION

1. Introduction

In the previous chapters it was assumed that all occurring particles were unpolarized, i.e. we have summed and averaged over all spin configurations. However, spins do play a dynamical role in the sense that the cross sections are usually different for different spin configurations, and measuring them can give additional information on the interactions under consideration. The spins of the incoming e^+e^- can in principle be influenced, which could for instance be used to give a relative enhancement of the weak interaction over the electromagnetic one in certain parts of phase space. Indeed, many papers have been published treating polarization effects on a variety of processes. We will again restrict ourselves to the effect of beam polarization on muon (or quark) pair production. The outline of this chapter is as follows: in section 2 transverse beam polarization is introduced, and it is shown how arbitrary beam polarization can be imposed on an event sample corresponding to unpolarized beams. Also an efficient algorithm is outlined to impose transverse beam polarization.

In section 3 it is indicated how the polarization of final state particles can be taken into account. Finally, the relevant formulae for muon and quark pair production for transversely polarized beams are given in section 4.

2. Beam polarization

It was realized already some time ago [1] that in e^+e^- accelerators the particles have a tendency to align their magnetic moments parallel to the magnetic field and hence become transversely polarized. The degree of polarization of a bunch of electrons (positrons) is defined as the difference in the numbers of spins pointing in the two alternative directions (in this case, the direction of the magnetic field, which is at right angles to the beams). Ideally, i.e. in case there are no depolarizing effects (like beam resonances) present, the degree of polarization P would increase as a function of time up to the theoretical maximum value P_0 as follows:

$$P(t) = P_0\left(1 - \exp(-t/t_0)\right) \qquad P_0 = 0.924$$

$$t_0 = 22\left[\frac{15 \text{ GeV}}{E_b}\right]^5 \text{ minutes} \qquad\qquad (7.1)$$

where the polarization time t_0 is a machine-dependent quantity. The number given
here holds for PETRA, and has comparable values for other large machines [2]. After
a time of roughly t_0, one could then perform polarization experiments. Due to
their very complicated structure, however, e^+e^- machines suffer from many
effects which may completely destroy the beam polarization. So far, only at
SPEAR transverse beam polarization has been seen in actual scattering processes [3].
None the less, much effort is being spent on obtaining polarization; by clever
manipulation of the beams it would then in principle be possible to obtain also
longitudinal polarization.

Since the electron is a spin-$\frac{1}{2}$ particle, its spin can assume two opposite
values along a fixed axis, for which we take the direction of the magnetic field,
assumed to be orthogonal to the ring plane. The colliding e^+e^- system can there-
fore be considered as a combination of four distinct spin configurations
(up + up , up + down , down + up and down + down). The measured cross section is a
weighted sum over the different configurations:

$$d\sigma(P) = \sum_{i=1}^{4} c_i(P)d\sigma_i .$$ (7.2)

The coefficients $c_i(P)$ are defined as the fraction of incoming e^+ and e^- that
have spins in the configuration i, in an experiment where the beams have a
degree of polarization P (not necessarily transverse). From this it follows
that the $c_i(P)$ are a partition of unity:

$$\sum_{i=1}^{4} c_i(P) = 1 .$$ (7.3)

It is easy to show that the polarizing weight $w(P)$, defined as

$$w(P) = d\sigma(P)/d\sigma(0)$$ (7.4)

has a finite maximum, given by

$$w(P) \leq 4 .$$ (7.5)

Depending on the degree of polarization P and possible symmetries in the inter-
actions which take place in the scattering process, such as CPT invariance, the
maximum may in practice even be smaller. Consequently, if we have generated an
event sample corresponding to the unpolarized cross section, we can modify it so
that polarization is taken into account. This can be done by applying a rejection
algorithm as in chapter VI. In this way a certain number of events from the
sample will be lost. Notice, however, that once a sample of unpolarized events has
geen generated, we can use it over and over to form samples corresponding to various
possible polarizations. The above method to simulate beam polarization in a sample
of generated events is applicable to both transversely and longitudinally polarized

beams. For the case of transverse polarization, however, there is another algorithm for imposing the polarization effect on the unpolarized event sample, without throwing away any of the events. This is derived from the observation that transverse polarization introduces a nontrivial dependence on the azimuthal angle in the cross section. If we integrate over this angle, however, any reference to the spin direction vanishes from the integral. Therefore, all the other phase space variables (energies and polar angles) must obey the same distributions as in the unpolarized case (after the azimuthal angle has been integrated over). The polarization can hence be implemented as follows:

- calculate the polarizing weight $w(P) = d\sigma(P)/d\sigma(0)$ for a given event;
- pick a random number η between 0 and the maximum possible weight;
- if $w(P)$ is larger than η, accept the event into the polarized event sample;
- if $w(P)$ is smaller than η, apply to the whole event a rotation around the beam axis over an arbitrary angle in $[0,2\pi]$, and try again.

In this way, the whole event sample is kept. It should be noted that, even if $P=0$, the new event sample will in general not be identical to the old one, since a number of events will have been rotated. Also, a given event sample can be 'depolarized' by applying an arbitrary rotation around the beam.

3. Polarization of the final state

The helicities of the particles that are produced in e^+e^- collision are in principle useful in extracting additional information on the interactions. This is especially true for the weak interactions, where helicity measurements could give very clean information on the right- or left-handedness of the weak gauge bosons. At present, however, the possibilities of determining the helicities are not very good. Only for τ pairs the helicity distributions can be determined in a statistical manner by examining the distribution of the decay products. In this section we describe how the helicities can be assigned to the produced particles after an event sample has been generated. In the measured cross section all spin configurations of the final state are present:

$$d\sigma = \sum_i d\sigma_i$$

where $d\sigma_i$ is the partial cross section corresponding to the configuration i. The helicities of a given event are now determined by the following algorithm:
- calculate for a given event the different quantities $d\sigma_i$;
- pick one of the spin configurations, using the $d\sigma_i$ as relative weights for this choice.

It is important that all particles are assigned a helicity simultaneously;

choosing the helicities of different particles independently can lead to incorrect correlations between the spins.

4. Cross sections for transversely polarized beams

In this last section we will present the cross sections for our example process, muon/quark pair production. Owing to our explicit use of the four currents defined in eq. (4.4) it becomes a trivial matter to include polarization in the formulae for the Born cross section and the virtual photon and soft bremsstrahlung corrections to it. The loop integrals that had to be calculated for section 3 of chapter IV do not depend on the spin of the external lines, and therefore the beam polarization is taken into account by modifying the current products of eq. (4.5):

$$|V \cdot V'|^2 = |V \cdot A'|^2 = s^2(1 + \cos^2\theta - P^2\sin^2\theta\cos2\phi)$$

$$|A \cdot V'|^2 = |A \cdot A'|^2 = s^2(1 + \cos^2\theta + P^2\sin^2\theta\cos2\phi)$$

$$(V \cdot V')(A \cdot A')^* = (V \cdot A')(A \cdot V')^* = 2s^2\cos\theta$$

$$(V \cdot V')(A \cdot V')^* = (V \cdot A')(A \cdot A')^* = P^2 i \, s^2\sin^2\theta\sin2\phi$$

$$(V \cdot V')(V \cdot A')^* = (A \cdot V')(A \cdot A')^* = 0 \tag{7.6}$$

where again P is the degree of polarization, and ϕ is the azimuthal angle of the μ^+ around the beam. The direction of the positron spin is defined to correspond to $\phi=0$. By inserting eq. (7.6) instead of eq. (4.5) into the expressions for the lowest order and virtual corrections (cf. eqs. (4.6-15)), we obtain the formulae for the case of polarized beams. As an illustration we give the expression for the Born cross section:

$$\frac{d\sigma_0(P)}{d\Omega} = \frac{\alpha^2 Q^2 Q'^2}{8s} \left[A(s)(1-\cos\theta)^2 + B(s)(1+\cos\theta)^2 + G(s)\sin^2\theta\cos2\phi \right.$$
$$\left. + H(s)\sin^2\theta\sin2\phi \right]$$

$$G(s) = -2P^2\left(1 + 2vv' \, \mathrm{Re}\, \chi(s) + (v^2-a^2)(v'^2+a'^2)|\chi(s)|^2\right)$$

$$H(s) = 4P^2 av' \, \mathrm{Im}\, \chi(s) . \tag{7.7}$$

It is seen that two new terms occur in the cross section, one of them depending on $\mathrm{Im}\,\chi(s)$. Therefore, the contribution of the soft bremsstrahlung will also contain such terms. Our approximation to the soft bremsstrahlung cross section is given by

$$\frac{d\sigma_s(P)}{d\Omega} = \frac{\alpha^2 Q^2 Q'^2}{8s} \left[\tilde{A}(s)(1-\cos\theta)^2 + \tilde{B}(s)(1+\cos\theta)^2 + \tilde{G}(s)\sin^2\theta\cos2\phi \right.$$
$$\left. + \tilde{H}(s)\sin^2\theta\sin2\phi \right]$$

$$\tilde{G}(s) = -2P^2\left[\delta_s^Q + 2vv' \ \text{Re} \ \chi(s)\delta_s^I + (v^2-a^2)(v'^2+a'^2)|\chi(s)|^2\delta_s^R \right]$$

$$\tilde{H}(s) = 4P^2 av' \ \text{Im} \ \chi(s)\delta_s^I \tag{7.8}$$

where the occurring quantities δ were already further defined in appendix A. Finally we have to calculate the cross section for hard bremsstrahlung. In principle, this can also be obtained from the same helicity amplitudes that were used to obtain eq. (4.18). The expression for the matrix element squared is as follows:

$$|M|^2(P) = 4e^6 Q^2 Q'^2 \left\{ Q^2 \left[\frac{1}{4k_+ k_- s'} \ \left(A(s')(t^2+t'^2) + B(s')(u^2+u'^2) \right. \right. \right.$$

$$+ G(s')(tu' \cos2\phi_+ + t'u \cos2\phi_-) + H(s')(tu' \sin2\phi_+ + t'u \sin2\phi_-))$$

$$- \frac{m_e^2}{2\kappa_+^2 s'^2} \ \left(A(s')t'^2 + B(s')u'^2 + G(s')t'u'\cos2\phi_- + H(s')t'u'\sin2\phi_- \right)$$

$$- \frac{m_e^2}{2\kappa_-^2 s'^2} \ \left(A(s')t^2 + B(s')u^2 + G(s')tu \cos2\phi_+ + H(s')tu \sin2\phi_+ \right)$$

$$\left. - \frac{m_e(k\cdot s)}{2s'^2\kappa_+^2} \ \left(J(s')t'^2+ K(s')u'^2\right) \ - \frac{m_e(k\cdot s)}{2s'^2\kappa_-^2} \ \left(J(s')t^2 + K(s')u^2 \right) \right]$$

$$+ Q'^2 \left[\frac{1}{4\kappa'_+ \kappa'_- s} \ \left(A(s)(t^2+t'^2) + B(s)(u^2+u'^2) \right. \right.$$

$$+ G(s)(tu' \cos2\phi_+ + t'u \cos2\phi_-) + H(s)(tu' \sin2\phi_+ + t'u \sin2\phi_-))$$

$$- \frac{m_\mu^2}{2s^2\kappa'^2_+} \ \left(A(s)t'^2 + B(s)u^2 + G(s)t'u \cos2\phi_- + H(s)t'u \sin2\phi_- \right)$$

$$\left. - \frac{m_\mu^2}{2s^2\kappa^2_-} \ \left(A(s)t^2 + B(s)u'^2 + G(s)tu' \cos2\phi_+ + H(s)tu' \sin2\phi_+ \right) \right]$$

$$+ QQ' \left[\frac{1}{4ss'} \left(\frac{u}{\kappa_+ \kappa'_-} + \frac{u'}{\kappa_- \kappa'_+} - \frac{t}{\kappa_+ \kappa'_+} - \frac{t'}{\kappa_- \kappa'_-} \right) \left(C(s,s')(t^2+t'^2) \right. \right.$$

$$+ D(s,s')(u^2+u'^2) + L(s,s')(tu' \cos 2\phi_+ + t'u \cos2\phi_-)$$

$$\left. + M(s,s')(tu' \sin2\phi_+ + t'u \sin2\phi_-) \right)$$

$$+ \frac{(s-s')M_z\Gamma_z}{2\kappa_+\kappa_-\kappa'_+\kappa'_-}\ \varepsilon_{\mu\nu\rho\sigma}p_+^\mu p_-^\nu q_+^\rho q_-^\sigma \cdot \left(E(s,s')(t^2-t'^2) - F(s,s')(u^2-u'^2) \right)$$

$$+ \frac{1}{2ss'}\ N(s,s') \left\{ \left(\frac{u}{\kappa_+\kappa'_-} + \frac{u'}{\kappa_-\kappa'_+} - \frac{t}{\kappa_+\kappa'_+} - \frac{t'}{\kappa_-\kappa'_-} \right) (tu'\ \sin 2\phi_+ - t'u\ \sin 2\phi_-) \right.$$

$$\left. - \frac{2(s-s')}{\kappa'_+\kappa'_-}\ \sqrt{tt'uu'}\ \sin(\phi_+ + \phi_-) + \frac{4t'u\ \sin 2\phi_-}{\kappa'_+} + \frac{4tu'\ \sin 2\phi_+}{\kappa'_-} \right\}$$

$$+ \frac{1}{2ss'}\ R(s,s') \left\{ \left(\frac{u'}{\kappa_+\kappa'_-} - \frac{u}{\kappa_-\kappa'_+} - \frac{t'}{\kappa_+\kappa'_+} + \frac{t}{\kappa_-\kappa'_-} \right) (tu'\ \cos 2\phi_+ - t'u\ \cos 2\phi_-) \right.$$

$$\left. \left. \left. - \frac{2(s-s')}{\kappa'_+\kappa'_-}\ \sqrt{tt'uu'}\ \cos(\phi_+ + \phi_-) + \frac{4t'u\ \cos 2\phi_-}{\kappa'_+} + \frac{4tu'\ \cos 2\phi_+}{\kappa'_-} \right\} \right] \right\}$$

$$J(s) = 2(av'-a'v)\ \text{Re}\ \chi(s) + 2\left(av(a'^2+v'^2) - a'v'(a^2+v^2) \right)|\chi(s)|^2$$

$$K(s) = 2(av'+a'v)\ \text{Re}\ \chi(s) + 2\left(av(a'^2+v'^2) + a'v'(a^2+v^2) \right)|\chi(s)|^2$$

$$L(s,s') = -2P^2\left(1 + vv'\ \text{Re}\big(\chi(s)+\chi(s')\big) + (v^2-a^2)(v'^2+a'^2)\ \text{Re}\big(\chi(s)\chi(s')^*\big) \right)$$

$$M(s,s') = 2P^2av'\ \text{Im}\ \big(\chi(s)+\chi(s')\big)$$

$$N(s,s') = P^2\left(a'v\ \text{Im}\big(\chi(s')-\chi(s)\big) + 2v'a'(v^2-a^2)\ \text{Im}\big(\chi(s')\chi(s)^*\big) \right)$$

$$R(s,s') = -P^2aa'\ \text{Re}\big(\chi(s')-\chi(s)\big)\ . \tag{7.9}$$

Here ϕ_+ and ϕ_- correspond to the azimuthal angle of the μ^+ and μ^- around the beam, respectively. If the photon is collinear to any other particle, these two angles differ by exactly $180°$. Upon integration over the azimuthal angle we recover the expression of eq. (4.18).

Notice in the above the occurrence of new terms which are proportional to only one power of m_e and P. At large polar scattering angle of the photon they can be neglected just like the mass terms that go with m_e^2, and for zero angle they vanish because of the overall factor of $(k\cdot s)$. However, they cannot be neglected if the scattering angle is of the order of $\sqrt{m_e/E_b}$, and are therefore included in our expression.

For the case of pure QED, which can be obtained by setting $\chi=0$, the expression for hard bremsstrahlung was first obtained by Kuraev et al. [4].

References

1. V.N. Baier, Usp. Fiz. Nauk 108 (1971) 1441, also Sov. Phys. Usp. 14 (1972)
    695.

2. For some comments on the detection of beam polarization, see e.g.
    P. Duinker, lectures given at the 18th International School of Subnuclear
    Physics at Erice, Italy 1980 (NIKHEF-H/81-05).

3. See, e.g. J.G. Learned, L.K. Resvanis, and C.M. Spencer, Phys. Rev. Lett.
    35 (1975) 1688.

4. E.A. Kuraev, M. Yu. Lel'chuk, V.S.Panin, and Yu.P. Persun'ko, Sov. J.
    Nucl. Phys. 32 (1980) 548.

CHAPTER VIII

APPLICATIONS

1. Introduction

We want to finish our treatment of the Monte Carlo approach to radiative
processes as presented in this thesis by giving an overview of the different
applications of this method in practice. We have argued in the second chapter
that event generators are necessary due to the fact (among other things) that
a realistic experimental situation seldom allows for a generally applicable
treatment. Therefore, the best illustrations of the method are just the
experimental results on the various distributions, compared to their
expectation as given by the computer simulation. Most of these have been made
public during the last few major conferences on high energy physics (1). Some
of the results presented here do not concern themselves with muon or quark
pair production, but rather with the processes $e^+e^+ \to e^+e^-$ (γ) and $e^+e^- \to \gamma\gamma$ (γ).
For these processes, also event generators have been constructed operating on
the principles outlined in the previous chapters (2). The other field where
event generators are of prime importance, the hadronization of quarks and
gluons into ordinary matter, is usually treated in a completely different
manner. We will not coment on any of those Monte Carlo results in this thesis.

We want to make one remark concerning the presentation of the radiative
corrections in the pictures given below. In principle, the experimental data
can be compared directly to the corrected prediction, e.g. the angular
distribution

$$\frac{d\sigma}{d\Omega} = \frac{d\sigma_0}{d\Omega} (1+\delta) , \qquad (8.1)$$

where $d\sigma_0/d\Omega$ is the nonradiative result, and δ the radiative correction. In
this case, the events generated in the computer simulation have been processed
in the experiment analysis just like the real data. On the other hand, once
the radiative correction is known, one can also modify the experimental
distribution so that it corresponds to the lowest order theoretical prediction,
by evaluating

$$\frac{d\sigma_{exp}}{d\Omega} = \frac{d\sigma_{exp}}{d\Omega} (1+\delta)^{-1} . \qquad (8.2)$$

The comparison is then made between (8.2) and $d\sigma_0/d\Omega$. It is the latter approach which is often chosen if the lowest order distribution has some simple and well-known form, like $1 + \cos^2\theta$ for QED muon pair production. Finally, the data are drawn with error bars; the Monte Carlo results are either presented as a histrogram or as a smooth curve, depending on whether so many events were used in the prediction that their statistical uncertainty is negligible.

2. Theory versus nature: comparison by means of the Monte Carlo method

In this section we will treat the different processes for which a computer simulation of the radiative effects has turned out to be useful in the last few years.

2.1. Beam luminosity

The process of Bhabha scattering $(e^+e^- \to e^+e^-)$ has a cross section which rises dramatically for very small scattering angles. Therefore, measurement of this reaction is considered the best way to determine the beam luminosity, simultaneously with the actual experiment. It is clear that a good understanding of the radiative effects are important here, because the luminosity enters into all other measured total cross sections. For specific and well-determined experimental set-ups, the cross section has been calculated by standard numerical integration (3). However, radiative Bhabha scattering has a very complicated cross section just in this region, and an accurate simulation is indispensable if a proposed luminosity measuring apparatus is to be tested or designed. (The same holds for a tagging system for two-photon processes, where it is in principle possible to go down to zero scattering angle (4)). As a result of careful simulation, discrepancies which existed between the luminosity determination from small and wide angle Bhabha scattering have disappeared (5).

2.2. Muon and tau pair production

The cross sections for muon and tau pair production have now been measured up to center-of-mass energies of about 37 GeV, resulting in no measurable deviation from the QED expectation. In fig. 10 the measured total cross sections have been plotted as a function of energy. In figs. 11 and 12 the angular distributions are given. In both results the QED effects have been taken into account up to order α^3, using event generators.

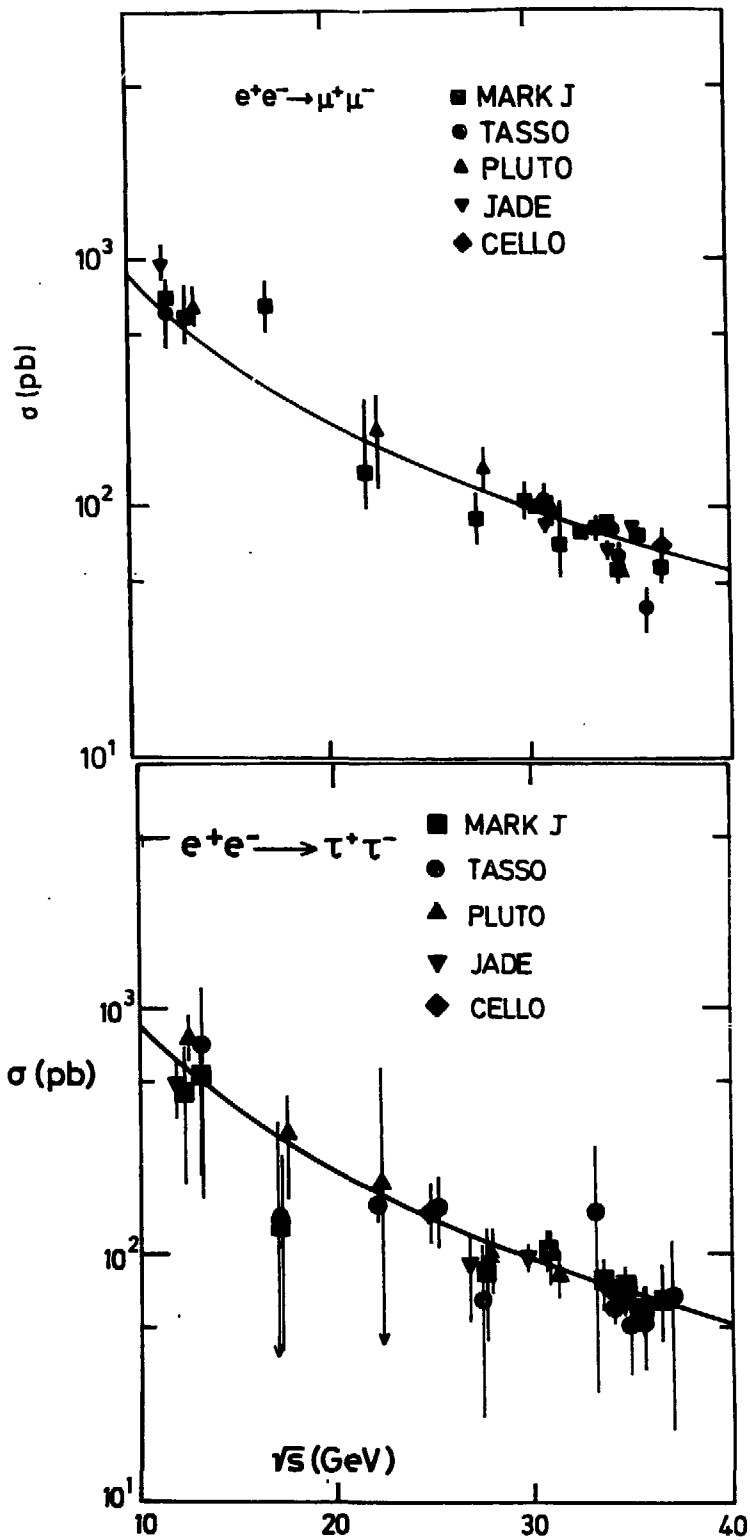This has been done following eq. (8.2). Also weak interaction effects, on
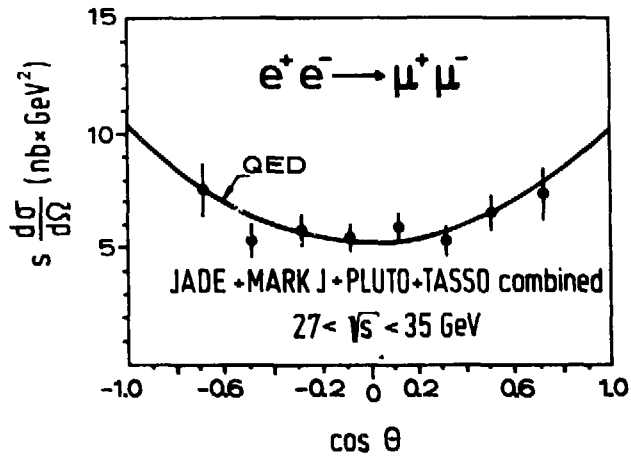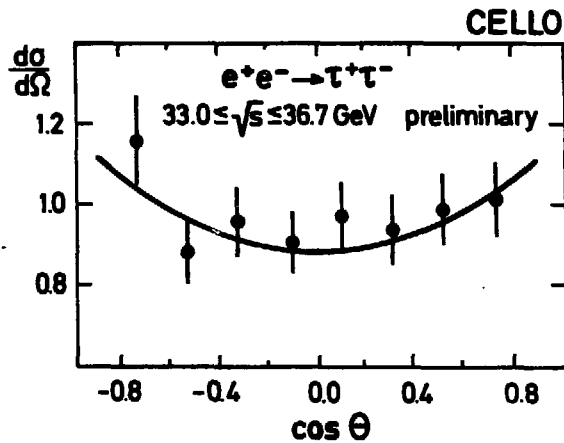
Fig. 10

Figure: Upper panel — $e^+e^- \rightarrow \mu^+\mu^-$ cross section σ (pb) versus $\sqrt{s}$ (GeV), with data from MARK J, TASSO, PLUTO, JADE, and CELLO. Lower panel — $e^+e^- \rightarrow \tau^+\tau^-$ cross section σ (pb) versus $\sqrt{s}$ (GeV), same experiments.

$$s\frac{d\sigma}{d\Omega}\ (nb\times GeV^2)$$

$$e^+e^-\longrightarrow \mu^+\mu^-$$

QED

JADE + MARK J + PLUTO + TASSO combined

$27 < \sqrt{s} < 35$ GeV

Fig. 11

CELLO

$$\frac{d\sigma}{d\Omega}$$

$$e^+e^-\rightarrow \tau^+\tau^-$$

$33.0\le \sqrt{s} \le 36.7$ GeV   preliminary

Fig. 12

which we will come back later, have been eliminated from the data. Extensive discussions of these results and their interpretation as checks of QED are given in refs. 6.

As stated in the previous chapter, the generation of τ pair production is complicated by the fact that the τ particles decay and only the decay products are measured. Their distribution is influenced by the τ helicity. To our knowledge, this has not been taken into account in a computer simulation so far.

2.3. *Bhabha scattering at large angles*

This process is, due to its higher statistics, probably an even better test of QED than those of the previous paragraph. In fig. 13 its angular distribution is shown. The same comments hold as for 2.2, but now eq. (8.1) has been followed.
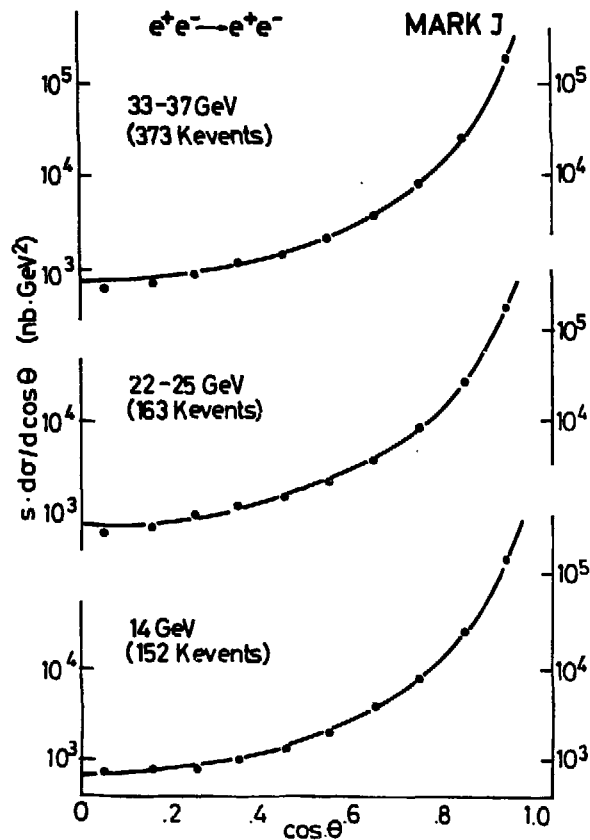
Fig. 13

2.4. *Electroweak interference*

The effect of weak interactions (mediated by the Z_0 boson) has been measured in muon and tau pair production and Bhabha scattering by subtracting from the data sample the background expected on the basis of pure QED (of course, also the quotient rather than the difference can be taken). Since the Z_0 resonance is still far above the presently available energies, these effects manifest themselves in practice only in the angular distributions. Since the higher-order QED contributions affect the angular distributions by

approximately the same amount (but with opposite sign for the case of muons), a very precise evaluation of these contributions is necessary. For muon pair production, the integrated forward-backward asymmetry has been determined to be $-7.7 \pm 2.4\%$ (DESY average) while the simple Glashow-Weinberg-Salam model (cf. chapter IV) would give a values of -7.8%. The corresponding value of $\sin^2\theta_w$ is $.24 \pm .07$ (7). This result is not at all as accurate as can be obtained in other experiments, but the $q^2 = s$ value at which the weak mixing angle has been measured is the highest reached so far.

In fig. 14 an angular distribution for muon pairs is compared to the pure QED expectation, using eq. (8.2). The solid line is a fit to the data, while the dashed line represents the $1 + \cos^2\theta$ behaviour expected for pure QED. In
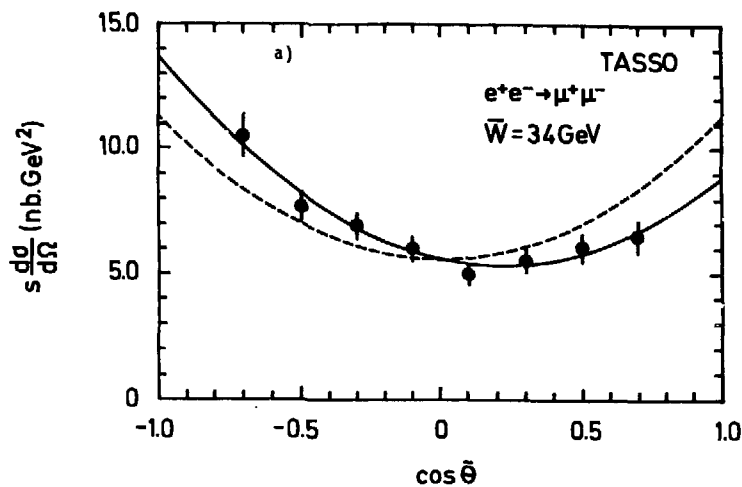
Fig. 14
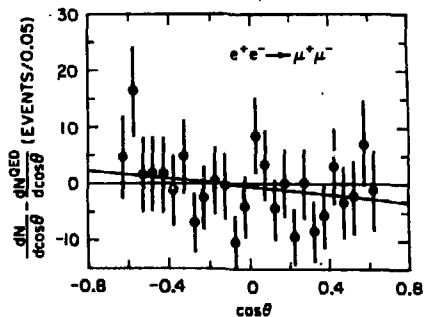
Fig. 15

this plot the data themselves where modified to eliminate the radiative effects. In fig. 15 the distribution for muon pairs is shown, where the QED

background has been subtracted. In fig. 16 similar pictures are given for Bhabha scattering, but this time the data are divided by the numbers expected from QED only. In these last two plots, eqs. (8.1) and (8.2) give the same results.
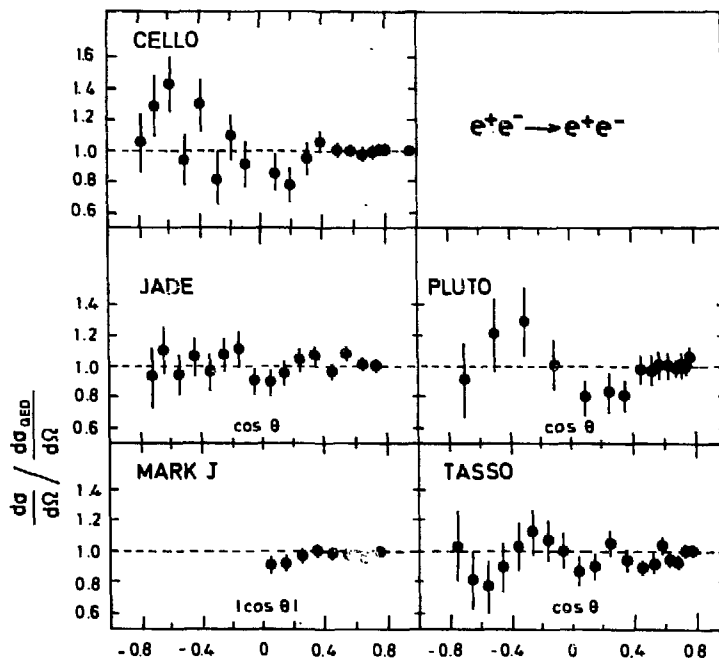

Fig. 16

2.5. *Hard bremsstrahlung in leptonic processes*

In case the bremsstrahlung photon is detected either by direct observation or by inferring its presence from e.g. the acoplanarity of the detected leptons, other quantities become observable, which themselves can again be considered tests of QED. Most important among these are the acollinearity (the angle made by the tracks of the muon pair or Bhabha pair, which is zero in case no photon was radiated) and the acoplanarity (the same angle, but now projected on the plane which goes through the interaction point at right angles to the e^+e^- beams). An acollinearity distribution is shown for Bhabha pairs in fig. 17, and an acoplanarity distribution for muon pairs in fig. 18. It may be interesting to notice that the events with nonzero acollinearity come mainly from bremsstrahlung by the incoming e^+e^-. A nonzero acoplanarity can only be caused by bremsstrahlung at large angles to both
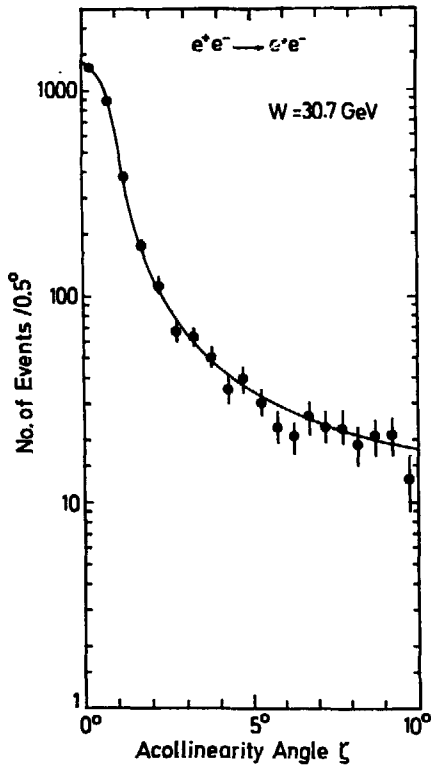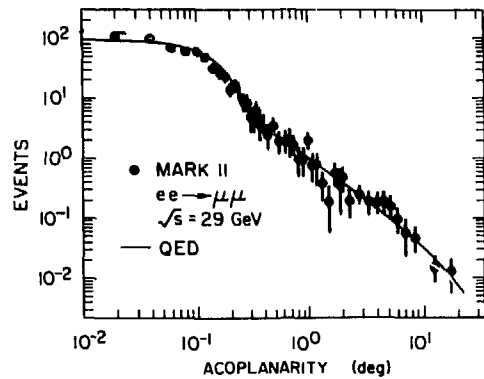
Fig. 17

Fig. 18

incoming and outgoing particles. Its distribution is therefore poorly described by the usual approximations, while trivial to obtain from an event generator. The good agreement of the data with the QED prediction gives also confidence in the differential cross sections mentioned in 2.1-4.

Hard bremsstrahlung events can also act as a background to nonstandard processes of which an example will be given in 2.8.

2.6. *Annihilation into photons*

Another of the 'standard' QED processes is the annihilation of e^+e^- into photons, mentioned in the introduction to this chapter. To lowest order in perturbation theory, two photons will be produced. Since this process is not influenced by weak or strong interaction effects in the next order in the coupling constant, it is an exceptionally clean test of QED in an experiment where neutral particles can be observed accurately. At LEP energies it may therefore be a better process with which the luminosity is measured than that of Bhabha scattering. The angular distribution is given in fig. 19, using eq. (8.1).
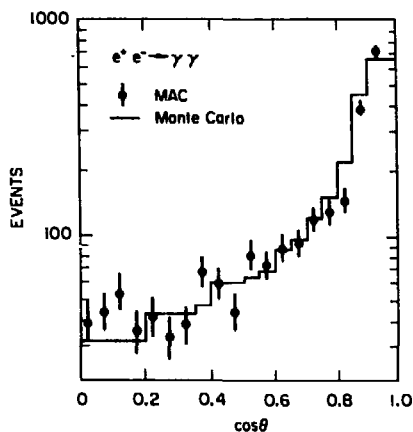
68

Fig. 19

The process $e^+e^- \rightarrow \gamma\gamma\gamma$ can be interpreted as the hard bremsstrahlung contribution to the two-photon annihilation. However, due to the fact that the three produced particles are indistinguishable, the bremsstrahlung phase space becomes very complicated for even a simple experimental setup (8). Also, the infrared divergence now occurs for every situation in which one of the photons becomes soft. These features make an integration over the cross section even more complicated than for the other leptonic processes. As is shown in ref. 2, these problems are circumvented in an elegant manner in the corresponding event generator. In fig. 20 the distribution of the energy of any of the three photons is shown for the case all three are produced at large angles to the beams.
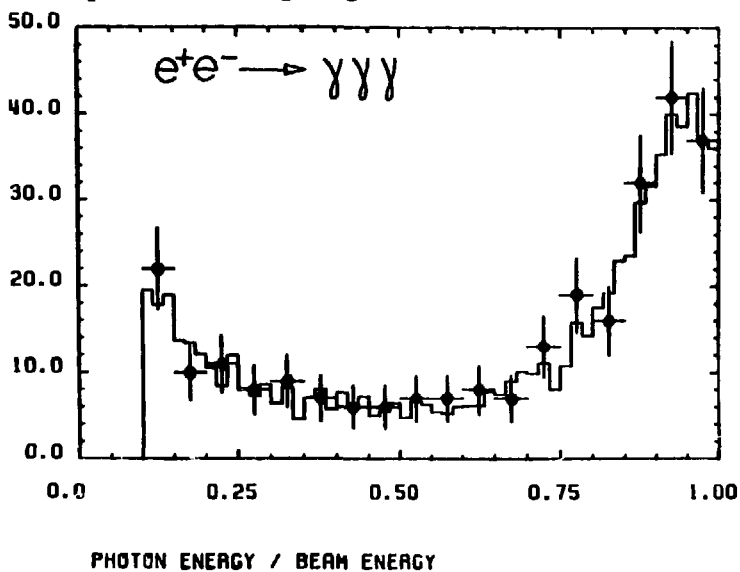

PHOTON ENERGY / BEAM ENERGY

Fig. 20

69

2.7. Bremsstrahlung in hadron production

The value of R, the ratio of the total cross section for hadron production to that for muon pair production, is one of the most important numbers obtained from e^+e^- experiments, since it directly measures the number of quarks that can be produced at a given centre-of-mass energy. In searches for new quarks it is quite possible that the narrow resonance corresponding to the S bound state of the quarks is missed by accident, but the increase in R above threshold can hardly be missed, if the new quark has charge 2/3 (for charge 1/3 quarks, the detection may be harder). Unfortunately, the accurate measurement of R is quite difficult. One of the largest effects in the measurement of R is that of hard bremsstrahlung from the initial e^+e^-, which can easily be of the order of 20% (9). Also any uncertainty in the beam luminosity enters directly in the systematic error.

In fig. 21 the value of R is given over the presently attainable energy range. The various resonances and steps in R, which signal the excitation of
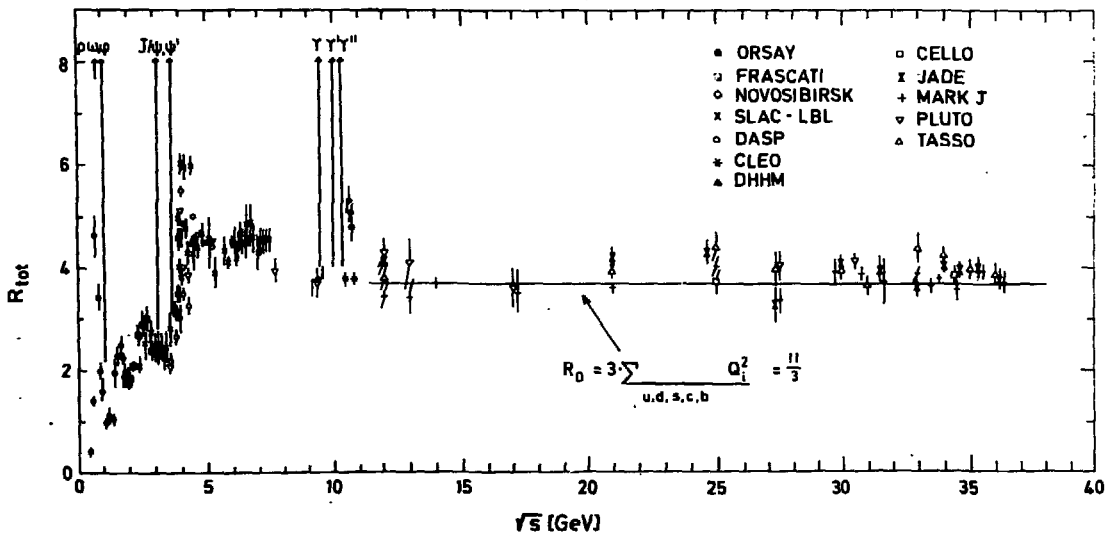

Fig. 21

new quark flavours can easily be seen.

Also of interest are the higher-order QCD corrections, which increase the measured value of R by a fraction $\alpha_s/\pi + O(\alpha_s^2)$. The first of these contributions is of the order of 6%, the second one of 2%. It is clear that if the order α_s^2 contribution is to be measured to any accuracy at all, the second-order QED effects, which are estimated to be about 3%, have to be known accurately as well.

The most accurate determination of the QCD coupling constant α_s is not the measurement of R, but rather the QCD equivalent of bremsstrahlung from the final state, in which a gluon instead of a photon is radiated. Ideally, the primordial quarks and the gluon decay into jets of hadrons, so that three jets are seen in the bremsstrahlung case, versus two jets in case no gluon is radiated. From the observed ratio of two- and three-jet events, the value of α_s can be extracted. In practice, however, two- and three-jet events may look quite similar, and also the distinction between the two is fundamentally arbitrary. The usual method to distinguish two- and three-jet events is therefore to characterize the topology of the hadronic event by one or more simple numbers, obtained by processing the measured hadronic momenta in some way. For this characterization of an event, a nearly infinite number of possibilities have been proposed. The recognition of four-jet events (and even higher) proceeds in the same way. The typical value of α_s obtained from this kind of analysis is $.17 \pm .01 \pm .03$ (DESY average, 1981). In methods of this kind, the QED effects enter in the following way. The initial e^+e^- have, as stated above, a quite large probability of emitting a high-energy photon. In that case, the produced hadrons will be boosted away from the interaction point in some direction (usually the direction of the beams; however, the assumption that this is always the case is not justified). A real two-jet event may then start to look like a three-jet event, certainly if the events are processed in order to obtain the characterizing numbers mentioned before. In this way, the number of three-jet events could for instance be overestimated. To avoid this, one has to use an event generator producing the correct amount of hard bremsstrahlung in a given direction, and another to generate the production and decay of the quarks, gluons and hadrons in the inertial frame resulting from the boost given by the hard photon. A detailed description of how this is done is given in chapter V. Extensive discussions of the analysis of hadronic events in order to obtain α_s can for instance be found in ref. (10).

2.8. *Excited leptons*

Apart from measurement of the 'standard' processes, much attention in e^+e^- collisions focuses on the discovery of new, 'nonstandard' phenomena. One of these is the existence of an excited state of leptons. Discovery of such a state would be a major development in our understanding of matter since it would imply a substructure in the leptons for which no evidence has been found at even the highest energies so far. Excited leptons would manifest themselves probably as heavy particles with the same charge as the 'ground-state'

leptons, and could decay into them by photon emission. Experimental searches have concentrated on excited partners of the electron and the muon. The best way to see an effect of an excited electron is the observation of deviations from QED in the process $e^+e^- \to \gamma\gamma$, where the excited electron e^* would be present with spacelike momentum in the t-channel. Consequently, the limits on its mass (and coupling constant) are given by the experimental correctness of QED for this process. Its existence is ruled out with high confidence at the present energies (12).

The discovery of an excited muon μ^* is only possible in radiative processes, the most likely of which are $e^+e^- \to \mu^*\mu^* \to \mu\mu\gamma\gamma$ and $e^+e^- \to \mu^*\mu \to \mu\mu\gamma$. It is clear that a heavy background to processes of this kind will come from the normal bremsstrahlung processes predicted by QED. Since there is no reason to expect that the decay $\mu^* \to \mu\gamma$ is very anisotropic, the photons coming from the μ^* events are probably seen best in quantities similar to the acoplanarity of paragraph 2.5. The result of such an analysis is given in fig. 22, where the invariant mass of any of the muons with the photon is plotted. An excited muon would cause in this plot a peak around the value of its rest mass. As can be seen, the plot exhibits no structure that cannot be
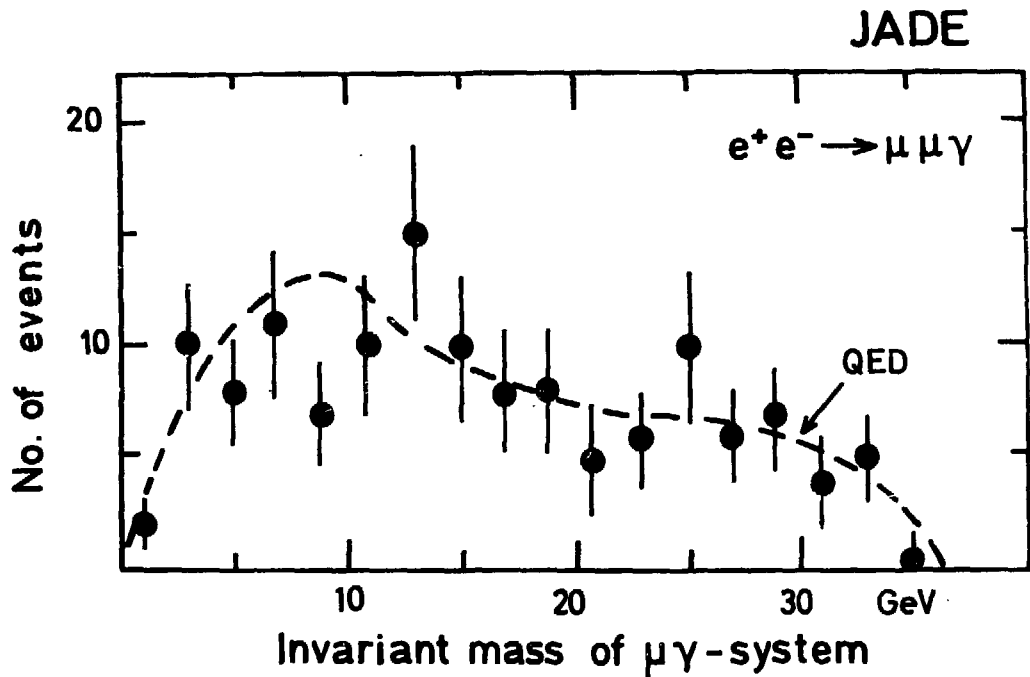

Fig. 22

explained by QED. At present, the existence of a μ^* is ruled out with good confidence, unless its mass is very large or its coupling very small.

A detailed treatment of similar searches is given in ref. (11).

3. Prospects

In the previous section we treated several applications of event generators for higher-order QED processes. In this section, some topics are given for which a similar method not yet exists, but can be obtained following the lines of this thesis.

3.1. *Two-photon physics*

For the process $e^+e^- \rightarrow e^+e^- X$ (X denoting a lepton pair, or hadrons), theoretical interest has always been considerable. Recently accurate experimental results have been obtained as well. Since the cross sections for processes of this kind do not decrease with energy like those in the one-photon channel, but instead rise logarithmically, they are expected to become more and more important as the available energies increase. Due to their complicated structure, the corresponding distributions are notoriously hard to predict. At present, the best way in which events for these processes are generated is by adapting a stratified-sampling Monte Carlo integration program in the way outlined in section 2 of chapter III (12). As remarked there, this approach has its drawbacks related to the weight distribution (cf. chapter VI) so it would certainly be worthwhile to construct a real event generator for this process. Special care would then be necessary because of the sharp peaking of distributions, and the spectacular numerical cancellations which sometimes occur in the cross section (a cancellation over 10 orders of magnitude is frequently seen). In particular the regions of small but not negligible scattering angles of the electrons (tagging mode) have to be simulated accurately.

3.2. *Radiative corrections to two-photon processes*

Unavoidably, the higher-order contributions to the processes in 3.1 will be important as soon as they are measured with reasonable accuracy. In particular it can be expected that small changes in the scattering angle of the e^+e^- due to bremsstrahlung can play an important role for measurements with single or double tagging. So far, only part of the radiative corrections

73

has been calculated, with very limited accuracy for the bremsstrahlung part
(13). The exact calculation of the complete virtual corrections (containing
many six-point loop integrals) and an accurate and fast event generation,
including the hard bremsstrahlung, would be a very interesting and important
accomplishment in view of the important role that the two-photon processes are
expected to play in future e^+e^- physics.

3.3. *Z-channel experiments*

At LEP/SPC energies many scattering processes will become observable for
which the present-day cross sections are far too small to measure. For all
these processes, event generators including radiative corrections will
probably be very useful. We mention here two possibilities only:

a. Neutrino counting.

The process $e^+e^- \rightarrow \gamma Z_0 \rightarrow \gamma \nu \bar{\nu}$, already mentioned in chapter II, is one
of the nicest ways to determine the number of (light) neutrinos, also
those that have charged leptonic partners that are too heavy to be
produced this way. This process can completely be simulated by the
initial state radiation formalism of chapter V. The most important
backgrounds to this process are Bhabha scattering and three-photon
annihilation. In fig. 23 these backgrounds are given as a function of
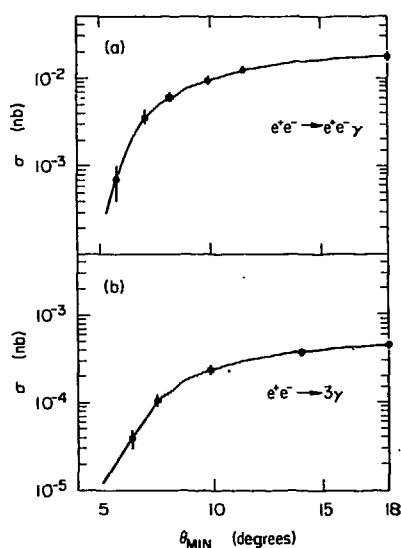the scattering angle of the photon under the condition that the other

Fig. 23

particles are close enough to the beams to disappear from the detector
(see also refs. 5 of chapter II).

In these pictures, the 'data points' are actually obtained using an event generator. The error bars indicate the statistical uncertainty on the Monte Carlo expectation, while the curve has been drawn smoothly through the points.

b. Higgs production

The discovery of the Higgs boson (if it exists at all) will be one of the most definite pieces of evidence for the Glashow-Weinberg-Salam model of the electroweak interactions. The most probable channel for its observation is $e^+e^- \rightarrow Z_0 \rightarrow Z_0H \rightarrow \mu^+\mu^-H$. Since the Higgs mass is unpredicted, it will enter as a parameter in fits made in the various distributions of the process $e^+e^- \rightarrow \mu^+\mu^- +$ (anything) (14). These distributions will of course be affected by the higher-order QED contributions. At present, the initial state radiation has been included (15). As soon as the process is actually observed, also final state radiation and the interference of the two will probably be of interest.

References

1. In the following 'Bonn' stands for:
   Proceedings of the 10th International symposium on lepton and photon interactions at high energies, Bonn 1981 (ed. W. Pfeil).
   'Wisconsin' stands for:
   Proceedings of the XXth International Conference on high energy physics, Madison 1980 (ed. L. Durand and

2. For e^+e^- into photons:
   F.A. Berends and R. Kleiss, Nucl.Phys. B186 (1981) 22.
   For e^+e^- into Bhabha pairs:
   F.A. Berends and R. Kleiss, unpublished.

3. F.A. Berends, K.J.F. Gaemers and R. Gastmans, Nucl.Phys. B68 (1974) 541.
   G. Ripken, unpublished.

4. See for instance the proposal for the ARGUS detector:
   H. Hasemann et al., DESY proposal no. 148.
   Also L. Jönsson, private communication.

5. J.P. Revol, private communication.

6. See, e.g. R. Hollebeek, Bonn, and J. Branson, Bonn.

7. J. Branson, Bonn.
   G. Wolf, DESY report 81-086.

8. F.A. Berends and R. Gastmans, Nucl. Phys. B61 (1973) 414.

9. F.A. Berends and R. Kleiss, Nucl.Phys. B177 (1981) 237.
   R. Felst, Bonn.

10. See, e.g. S.L. Wu, Wisconsin, and H.B. Newman, Wisconsin.

11. J. Bürger, Bonn.

12. See, e.g. S. Kawabata, as quoted by J.H. Field on the 4th International
    colloquium on photon-photon interactions, Paris 1981 (ed. G.W. London).

13. S. Defrise, Z.f. Phys. C9 (1981) 41.

14. J. Ellis et al., Nucl.Phys. B106 (1975) 292.
    D.R.T. Jones and S. Petcov, Phys.Lett. 84B (1979) 440.
    R.L. Kelly and T. Shimada, Phys.Rev. D28 (1981) 1940

15. F.A. Berends and R. Kleiss, Leiden preprint (to be published).

References to the pictures

The figures were taken from the following sources:
Figs. 10, 12, 13: J. Branson, Bonn
Fig. 11: B.H. Wiik, DESY report 80-129
Fig. 14: TASSO collaboration, DESY report 82-002.
Figs. 15, 18, 19: R. Hollebeek, Bonn.
Figs. 16, 17: G. Wolf, DESY report 81-086.
Fig. 20: H. Takeda, private communication (JADE collaboration)
Fig. 21: R. Felst, Bonn.
Fig. 22: J. Bürger, Bonn.
Fig. 23: G. Barbiellini et al., Phys.Lett. 106B (1981) 414.

Appendix A

We give here the formulae describing the virtual and soft bremsstrahlung corrections for muon pair production which were introduced in chapter IV. Since all of these, except the formulae for soft bremsstrahlung, have been known for quite some time, no derivation is given, but instead we refer to the literature.

Vertex correction (eq. 4.8)

$$F(s,m^2) = \frac{1}{4\pi^2} \left\{ \left(\ln \frac{s}{m^2} - 1 \right) \ln \frac{\lambda}{m} - \frac{1}{4} \ln^2 \frac{s}{m^2} + \frac{3}{4} \ln \frac{s}{m^2} + \frac{\pi^2}{3} - 1 \right\} . \qquad (A.1)$$

In the ultrarelativistic limit, F has no imaginary part (1). λ is the infinitesimally small photon mass introduced in chapter IV.

Vacuum polarization (eq. 4.9)

$$\text{Re } \Pi_i(s) = \frac{\alpha}{\pi} Q_i^2 \left\{ - \frac{1}{3} \ln \frac{s}{m_i^2} + \frac{5}{9} \right\}$$

$$\text{Im } \Pi_i(s) = \frac{\alpha}{3} Q_i^2 \qquad\qquad i = e,\mu,\tau . \qquad\qquad (A.2)$$

These formulae hold for any (light) fermion, so also quark masses could be inserted here if they were known. See also ref. (1).

Box diagram with two photons (eq. 4.12)

$$V_1 = \frac{1}{8\pi^2} \left\{ -8 \ln \left(\frac{a}{b} \right) \ln \frac{2E_b}{\lambda} - c \left(\frac{\ln^2 a}{b^4} + \frac{\ln^2 b}{a^4} \right) + \frac{\ln a}{b^2} - \frac{\ln b}{a^2} \right\}$$

$$V_2 = \frac{1}{16\pi^2} \left\{ 4\ln(\frac{a}{b}) - c \left(\frac{\ln a}{b^4} + \frac{\ln b}{a^4} \right) - \frac{2c}{1-c^2} \right\}$$

$$A_1 = \frac{1}{8\pi^2} \left\{ -c \left(\frac{\ln^2 a}{b^4} - \frac{\ln^2 b}{a^4} \right) + \frac{\ln a}{b^2} + \frac{\ln b}{a^2} \right\}$$

$$A_2 = \frac{1}{16\pi^2} \left\{ -c \left(\frac{\ln a}{b^4} - \frac{\ln b}{a^4} \right) + \frac{2}{1-c^2} \right\} \qquad\qquad (A.3)$$

where the quantities a, b and c are defined as

$$a = \sin \frac{\theta}{2} , \quad b = \cos \frac{\theta}{2} , \quad c = \cos\theta . \qquad\qquad (A.4)$$

See also ref. (2).

Box diagram with one photon and one Z_o (eq. 4.13)

$$\text{Re } \delta_{zY} = \frac{1}{4\pi^2} \left\{ -2 \ln(\frac{a}{b}) \ln\left[\frac{(s-M_z^2)^2 + M_z^2\Gamma_z^2}{M_z^2\lambda^2} \right] \right.$$

$$\left. + 2\ln^2 b - 2\ln^2 a + \text{Li}_2(a^2) - \text{Li}_2(b^2) \right\}$$

$$\text{Im } \delta_{zY} = \frac{1}{\pi^2} \ln(\frac{a}{b}) \arctan\left(\frac{M_z\Gamma_z}{M_z^2-s} \right) . \tag{A.5}$$

The dilogarithm function $\text{Li}_2(x)$ is defined as

$$\text{Li}_2(x) = - \int_0^x dy \, \frac{1}{y} \ln(1-y) \tag{A.6}$$

and has the following series expansion for $x<1$:

$$\text{Li}_2(x) = \sum_{k=1}^{\infty} \frac{x^k}{k^2} , \quad \text{Li}_2(1) = \frac{\pi^2}{6} . \tag{A.7}$$

In eq. (A.5) the arctan is defined to be continuous at $s=M_z^2$, i.e.

$$-\infty < x < 0 : \frac{\pi}{2} < \arctan(x) < \pi$$

$$0 < x < \infty \quad : 0 < \arctan(x) < \frac{\pi}{2} . \tag{A.8}$$

See also ref. (2).

For completeness, we give here the expression for the interference of M_0 and M_v, as mentioned in eq. (4.15):

$$\text{Re } M_0 M_v^* = \frac{e^6 Q^2 Q'^2}{s^2} \times \left\{ QQ' \left[A_1 \text{ Re}\left((V \cdot V')(A \cdot A')^*\right) + 2\pi A_2 \text{ Im}\left((V \cdot V')(A \cdot A')^*\right) \right] \right.$$

$$+ |V \cdot V'|^2 \left[Q^2 F(s,m_e^2) + Q'^2 F(s,m_\mu^2) - \frac{1}{e^2} \text{Re } \Pi(s) + QQ'V_1 \right]$$

$$+ |\chi(s)|^2 |(vV+aA) \cdot (v'V'+a'A')|^2 \left[Q^2 F(s,m_e^2) + Q'^2 F(s,m_\mu^2) + QQ' \text{ Re } \delta_{zY} \right]$$

$$+ \text{Re}\left((vV+aA) \cdot (v'V'+a'A')(V \cdot V')^*\right) \left[2\text{Re } \chi(s)\left(Q^2 F(s,m_e^2) + Q'^2 F(s,m_\mu^2)\right) \right.$$

$$- \frac{1}{e^2} \text{Re } \chi(s) \text{ Re } \Pi(s) - \frac{1}{e^2} \text{ Im } \chi(s) \text{ Im } \Pi(s)$$

$$+ QQ'\left(V_1 \text{Re } \chi(s) + 2\pi V_2 \text{ Im } \chi(s) + \text{Re } \delta_{zY} \text{ Re } \chi(s) - \text{Im } \delta_{zY} \text{ Im } \chi(s)\right) \Big]$$

$$+ \text{Im}\left((vV+aA) \cdot (v'V'+a'A')(V \cdot V')^*\right) \left[-2\text{Im} \chi(s)\left(Q^2 F(s,m_e^2) + Q'^2 F(s,m_\mu^2)\right) \right.$$

$$+ \frac{1}{e^2} \text{Im } \chi(s) \text{ Re } \Pi(s) - \frac{1}{e^2} \text{Re } \chi(s) \text{ Im } \Pi(s)$$

$$- QQ' \Big[V_1 \text{ Im } \chi(s) - 2\pi V_2 \text{Re } \chi(s) + \text{Re } \delta_{z\gamma} \text{ Im } \chi(s) + \text{Im } \delta_{z\gamma} \text{ Re } \chi(s) \Big) \Big]$$

$$+ \text{Re} \Big((vV+aA) \cdot (v'V'+a'A')(A \cdot A') \Big) QQ' \Big(A_1 \text{ Re } \chi(s) + 2\pi A_2 \text{ Im } \chi(s) \Big)$$

$$+ \text{Im } \Big((vV+aA) \cdot (v'V'+a'A')(A \cdot A') \Big) QQ' \Big(-A_1 \text{ Im } \chi(s) + 2\pi A_2 \text{ Re } \chi(s) \Big) \Big\} \qquad (A.9)$$

Soft bremsstrahlung (eq. 4.17)

$$\delta_s^Q = (\beta_i + \beta_f + 2\beta_{int}) \ln \frac{2E_0}{\lambda}$$

$$+ \frac{2\alpha}{\pi} Q^2 \left[-\frac{1}{4} \ln^2 \frac{s}{m_e^2} + \frac{1}{2} \ln \frac{s}{m_e^2} - \frac{\pi^2}{6} \right] + \frac{2\alpha}{\pi} Q'^2 \left[-\frac{1}{4} \ln^2 \frac{s}{m_\mu^2} + \frac{1}{2} \ln \frac{s}{m_\mu^2} - \frac{\pi^2}{6} \right]$$

$$+ \frac{2\alpha}{\pi} QQ' \left[2\ln^2 a - 2\ln^2 b - \text{Li}_2(a^2) + \text{Li}_2(b^2) \right]$$

$$\delta_s^I = \delta_s^Q + (\beta_i + \beta_{int}) \left(\frac{1}{2} \left(\frac{\zeta^2 + \gamma^2}{\zeta} - 1 \right) \psi - \frac{\gamma}{\zeta} \phi \right)$$

$$\delta_s^R = \delta_s^Q + \beta_i \left(\frac{1}{2} (\zeta^2 + \gamma^2 - 1) \psi + \frac{1}{\gamma} \left((\zeta^2 + \gamma^2)(\zeta-2) + \zeta \right) \phi \right)$$

$$+ 2\beta_{int} \left(\frac{1}{2} (\zeta-1) \psi - \gamma \phi \right)$$

$$\beta_i = \frac{2\alpha}{\pi} Q^2 \left(\ln \frac{s}{m_e^2} - 1 \right), \quad \beta_f = \frac{2\alpha}{\pi} Q'^2 \left(\ln \frac{s}{m_\mu^2} - 1 \right), \quad \beta_{int} = \frac{4\alpha}{\pi} QQ' \ln\left(\frac{a}{b}\right),$$

$$(A.10)$$

where

$$\psi = \ln \frac{(E_0/E_b - \zeta)^2 + \gamma^2}{\zeta^2 + \gamma^2}$$

$$\phi = \arctan\left(\frac{E_0/E_b - \zeta}{\gamma} \right) - \arctan\left(-\frac{\zeta}{\gamma} \right)$$

$$\zeta = 1 - M_z^2/s$$

$$\gamma = M_z \Gamma_z / s . \qquad (A.11)$$

In eq. (A.11) the arctan is defined to be continuous at $E_0 = \zeta E_b$, i.e.

$$-\infty < x < 0: \quad -\frac{\pi}{2} < \arctan(x) < 0$$

$$0 < x < \infty: \quad 0 < \arctan(x) < \frac{\pi}{2} . \qquad (A.12)$$

The expression (A.10) was first introduced in ref. (3). Before concluding this appendix, we want to remark that it is essential that the correct branches

for the two occurring arctangents are chosen. For very narrow resonances like
the J/ψ the two can be identified up to a constant, but for the Z_0 this is not
the case any more. Since in the soft bremsstrahlung formulae the arctangent
function is the dominant part of the contribution for values of s just above
M_z^2, any error here will result in a grossly overestimated soft photon effect.
As an example, all formulae occurring in ref. (4) are completely correct, but
the numerical results for $d\sigma_v/d\Omega$ differ greatly from our figs. 8.

References

1. The complete expressions containing all masses can be found in G. Källén,
    Handb. d. Phys., ed. S. Flugge (Springer, Berlin 1958), vol. 5 p. 304.
    The ultrarelativistic limits used here are from
    F.A. Berends and R. Gastmans, in: Electromagnetic Interactions of Hadrons,
    ed. A. Donnachie and G. Shaw (Penum, 1978).

2. I.B. Kriplovich, Sov.J.Nucl.Phys. 17 (1973) 298.
    G. Altarelli, R. Petronzio, and R.K. Ellis, Nuovo Cim.Lett. 13 (1975) 393.
    A.B. Kraemmer and B. Lautrup, Nucl.Phys. B95 (1975) 380.
    F.A. Berends, K.J.F. Gaemers and R. Gastmans, Nucl.Phys. B63 (1973) 381.

3. F.A. Berends, R. Kleiss and S. Jadach, ref. 3 of chapter IV.

4. M. Greco et al., Nucl.Phys. B171 (1980) 118.

Appendix B

In this appendix the formulae for the total approximate hard photon cross
sections are given. For initial state radiation, we obtain upon integrating
eq. (5.8):

$$\int_{k_1}^{k_2} dk^0 \frac{d\sigma_I}{dk^0} = \frac{\alpha}{\pi} Q^2 \left(\ln \frac{s}{m_e^2} - 1\right) \left(F_i(k_2/E_b) - F_i(k_1/E_b)\right)$$

$$F_i(x) = h_1 \ln x - \ln(1-x) + h_2 x + h_3 \ln\left((x-\zeta)^2 + \gamma^2\right) + h_4 \arctan\left((x-\zeta)/\gamma\right).$$

$$(B.1)$$

The coefficients h_i are defined as follows:

$$h_1 = 2\left(1 + (c_2\zeta + c_3)/(\zeta^2 + \gamma^2)\right)$$

$$h_2 = -(1 + c_2 + c_3)$$

$$h_3 = c_2\left(\frac{1+\mu}{2} - \zeta/(\zeta^2+\gamma^2)\right) + c_3\left(\frac{1}{2} + \mu - 1/(\zeta^2+\gamma^2)\right)$$

$$h_4 = c_2\gamma\left(1 - 2/(\zeta^2+\gamma^2)\right) + c_3\frac{1}{\gamma}\left(2\zeta/(\zeta^2+\gamma^2) - 2 - \mu - \mu^2 + \gamma^2\right) \qquad \text{(B.2)}$$

with the quantities ζ and γ as in appendix A, and

$$\mu = 1 - \zeta$$

$$c_2 = 2vv'$$

$$c_3 = (v^2 + a^2)(v'^2 + a'^2) \ . \qquad \text{(B.3)}$$

For final state radiation, we obtain

$$\int_{k_1}^{k_2} dk^0 \frac{d\sigma_F}{dk^0} = \frac{\alpha}{\pi} Q'^2 \sigma_0(s)\left(F_f(k_2/E_b) - F_f(k_1/E_b)\right)$$

$$F_f(x) = \ln\left(\frac{s}{m_\mu^2}\right)\left(2\ln x - 2x - \frac{1}{2}x^2\right) - 2\text{Li}_2(x)$$

$$+ \left(\frac{3}{2} - 2x + \frac{1}{2}x^2\right)\ln(1-x) + \frac{3}{2}x - \frac{3}{4}x^2 \qquad \text{(B.4)}$$

where the dilogarithm Li_2 was also introduced in appendix A.

SAMENVATTING

Gedurende de laatste tien jaar hebben experimenten met botsende electron-
positron bundels een vooraanstaande rol gespeeld in de studie van elementaire
deeltjes. Niet alleen hebben zij het bestaan van nieuwe deeltjes vastgesteld,
waaronder de twee nieuwe quarks, het gluon en het τ-lepton, maar ook is het
mogelijk gebleken via deze weg gedetailleerde quantitative informatie te ver-
krijgen omtrent de wisselwerkingen tussen de deeltjes. Met name kunnen theo-
rieën omtrent electromagnetische en zwakke wisselwerkingen enerzijds, en sterke
wisselwerking anderzijds, beproefd worden tot op zeer kleine afstanden.

Sinds de introductie van de grootste e^+e^- machines (PETRA, PEP) is een
begin gemaakt met het nauwkeurig meten van kleine maar uiterst belangrijke ef-
fecten (zoals de voor-achterwaartse asymmetrie in muon paar productie, en de
observatie van drie-jet events in hadron productie) waaruit direct informatie
kan worden afgeleid omtrent de fundamentele natuurwetten en hun eventuele
samenhang in een geünificeerde veldentheorie.

Bij de analyse van dergelijke experimenten is een grondige kennis van de
resultaten, die men kan verwachten op grond van de theorie, van essentiëel
belang. Met name de hogere-orde bijdragen tengevolge van de quantum-electro-
dynamica (QED), die vaak van dezelfde orde van grootte zijn als de te meten
nieuwe effecten, dienen op een correcte wijze in rekening te worden gebracht.

In dit proefschrift wordt uiteengezet hoe men de hogere-orde QED bijdragen,
de zgn. stralingscorrecties, op een uiterst elegante en conceptueel eenvoudige
wijze in de analyse van het experiment kan introduceren. Hiertoe wordt gebruik
gemaakt van de techniek van Monte Carlo simulaties. Deze methode, die bij uit-
stek geschikt is voor het bestuderen van stochastische processen (waarbij de
afzonderlijke gebeurtenissen onvoorspelbaar zijn, maar de kans op het optreden
van een gebeurtenis nauwkeurig bepaald is), werd in deze vorm slechts in be-
perkte mate gebruikt voor het simuleren van e^+e^- botsingen. Met name het pro-
bleem van de stralingscorrecties stelt aan de simulatie hoge eisen, zowel wat
betreft de exacte vorm van de na te bootsen waarschijnlijkheidsverdeling
(waarbij aanmerkelijke numerieke complicaties kunnen voorkomen), als aan de te
volgen strategie.

In het proefschrift wordt een algemene techniek ontwikkeld om dit soort
problemen aan te pakken. Als illustratie wordt een algorithme ontwikkeld om de
processen van muon paar-produktie en quark paar-produktie te simuleren. Tevens
wordt een eenvoudige methode beschreven om dezelfde processen te bestuderen in
het geval dat de e^+e^- bundels transversaal gepolarizeerd zijn.

Met behulp van de beschreven technieken kunnen computerprogramma's ontwikkeld worden die de botsingsprocessen nabootsen door op een stochastische manier waarden van energie en impuls van de in de botsing geproduceerde deeltjes te geven en n waarschijnlijkheid die de stralingscorrecties insluit. Het is dan mog. . . k een groot aantal van deze sets van energieën en impulsen ("events") te verzamelen. Daarna kunnen deze op precies dezelfde wijze geanalyseerd worden als in het werkelijke experiment. Het voordeel van deze methode is dat ze uiterst flexibel is: elke grootheid die experimenteel gedefinieërd kan worden, kan in principe berekend worden uitgaande van dezelfde verzameling events.

In het laatste hoofdstuk worden enkele resultaten van de vergelijking tussen experiment en theorie gegeven. Uit het feit dat de betreffende voorspellingen alle gebaseerd zijn op simulatieprogramma's geconstrueerd volgens de in dit proefschrift aangegeven lijnen, blijkt het succes van de Monte Carlo methode als een van de meest hanteerbare en accurate methodes om tot experimenteel toegankelijke consequenties van de theorie te komen.

CURRICULUM VITAE

Ronald Kleiss, geboren op 16 februari 1955 te Schiedam, behaalde in 1973 het einddiploma Gymnasium aan de Spieringshoek Scholengemeenschap. Hierna studeerde hij natuurkunde aan de Rijksuniversiteit te Leiden, hetgeen resulteerde in het kandidaatsexamen met bijvak sterrenkunde in 1976, en het doctoraalexamen met bijvak wiskunde en onderwijsbevoegdheid in 1978. Tijdens zijn studie verrichtte hij experimenteel werk in de groep van Prof.Dr. R. de Bruyn Ouboter. In het kader van een beleidsruimteproject trad hij in oktober 1978 toe tot de werkgroep H-Th-L van de Stichting voor Fundamenteel Onderzoek der Materie. Onder leiding van Prof.dr. F.A. Berends verrichtte hij op het Instituut-Lorentz voor Theoretische Natuurkunde onderzoek op het gebied van de hoge-energiefysica en de veldentheorie; verder vervulde hij enige onderwijstaken. In verband met de bovengenoemde onderzoekingen maakte hij verschillende buitenlandse reizen, waaronder naar DESY (Hamburg), SLAC (Stanford, CA) en Cornell University (Ithaca, NY). Verder nam hij deel aan de zomerschool over ijktheorieën te Les Houches in 1981.

LIJST VAN PUBLIKATIES

1. F.A. Berends and R. Kleiss:
    Distributions in the process $e^+e^- \to \mu^+\mu^-(\gamma)$.
    Nucl.Phys. B177 (1981) 237.

2. F.A. Berends and R. Kleiss:
    Initial state radiation for e^+e^- annihilation into jets.
    Nucl.Phys. B178 (1981) 141.

3. F.A. Berends and R. Kleiss:
    Distributions for electron-positron annihilation into two and three
    photons.
    Nucl.Phys. B186 (1981) 22.

4. F.A. Berends, R. Kleiss, P. de Causmaecker, R. Gastmans, and T.T. Wu:
    Multiple bremsstrahlung processes in gauge theories.
    Phys.Lett. 103B (1981) 124.

5. F.A. Berends, R. Kleiss and S. Jadach.
    Radiative corrections to muon pair and quark pair production in electron-
    positron collisions in the Z_0 region.
    Leiden preprint (to be published in Nucl.Phys. B).

6. F.A. Berends, R. Kleiss and S. Jadach.
    Monte Carlo simulation of radiative corrections to the processes $e^+e^- \to \mu^+\mu^-$
    and $e^+e^- \to \bar{q}q$ in the Z_0 region.
    Leiden preprint.

7. F.A. Berends, R. Kleiss, P. de Causmaecker, R. Gastmans, W. Troost and
    T.T. Wu:
    Multiple bremsstrahlung in gauge theories at high energies II: single
    bremsstrahlung.
    Leiden preprint (to be published in Nucl.Phys. B).

8. F.A. Berends and R. Kleiss:
    Radiative effects in Higgs production at LEP.
    Leiden preprint.

ACKNOWLEDGEMENTS

The picture appearing on the cover is identical to fig.22 of chapter VIII.

STELLINGEN

1. De Miura transformatie, voor de cylindrische Korteweg - de Vries verge-
   lijking "by trial and error" gevonden door Nakamura, kan zonder trial
   and error direct worden afgeleid uit de eerder door hemzelf aangegeven
   Bäcklund transformatie.

   A.Nakamura, Journ.Phys.Soc.Japan 49 (1980) 2380
   A.Nakamura, Phys.Lett. 82A (1981) 111

2. De door Bedeaux en Mazur gebruikte methode om de stabiliteit van statio-
   naire oplossingen van het zogenaamde "hot spot" model te bestuderen,
   kan gegeneraliseerd worden voor niet-stationaire oplossingen. Op grond
   hiervan mag men aannemen dat discrepantie tussen numerieke en analytische
   resultaten voor dit model niet kunnen worden verklaard uit het bestaan
   van periodieke oplossingen met zeer kleine limietcykels.

   D.Bedeaux en P.Mazur, Journ.Stat.Phys. 24 (1981) 215 en Physica 105A
   (1981) 1

3. De wijze waarop Shuler en Mohanty het tellen van roosterbindingen in
   irreducibele roosterfragmenten toepassen ter berekening van de effectieve
   diffusieconstante voor random wandelingen op roosters met vallen is onjuist.

   K.E.Shuler, Physica 95A (1979) 12
   K.E.Shuler en U.Mohanty, La Jolla preprint, te publiceren in Proc.North
   Atl.Ac.Sci.

4. Het verband tussen "infrarode" en "collineaire" divergenties in rem-
   stralingsprocessen kan op eenvoudige wijze worden aangetoond.

   Hoofdstuk I van dit proefschrift

5. De nauwkeurigheid van de zogenaamde Weiszäcker – Williams benadering in
   twee-foton processen kan geschat worden door de bijdragen te vergelijken
   van termen die in deze benadering worden meegenomen en van verwaarloosde
   termen. Hieruit blijkt dat voor lage invariante massa van het fotonpaar
   iedere overeenkomst t..ssen de voorspellingen op grond van deze benadering
   en het exacte resultaat berust op toeval.

6. In e^+e^- botsingsprocessen waarin het electron-positronpaar annihileert in
   één virtueel foton kan de differentiële botsingsdoorsnede voor het proces
   waarin het e^+e^- paar een remstralingsfoton uitzendt op eenvoudige wijze
   worden uitgedrukt in de differentiële botsingsdoorsnede voor het proces
   zonder remstraling. Deze behandelingswijze kan zonder meer worden over-
   genomen voor het geval dat het electron-positronpaar annihileert in een
   Z_0 boson.

7. Zij $\vec{p}$ de impuls van een klassiek vrij puntdeeltje met massa m, en zij
   $E(|\vec{p}|)$ de corresponderende energie, waarvoor in de limiet van kleine $\vec{p}$
   asymptotisch geldt: $E(|\vec{p}|) = E(0) + |\vec{p}|^2/(2m)$. Laten $E(|\vec{p}|)$ en $\vec{p}$ worden
   opgevat als de componenten van een vector in een vierdimensionale vector-
   ruimte V. Laat $(E(0),0)$ overgevoerd worden in $(E(|\vec{p}|),\vec{p})$ door een matrix
   $M(\vec{p})$ waarvoor geldt:
   1) $M(\vec{p})$ laat elke vector $(0,\vec{q})$ invariant waarvoor $\vec{p}.\vec{q} = 0$;
   2) $M(\vec{p})$ voert $(E(|\vec{p}|), -\vec{p})$ over in $(E(0),0)$;
   3) voor reële x vormt de verzameling van alle $M(x\vec{p})$ een groep.
   Dan is de enige reële symmetrische bilineaire vorm op V, die invariant is
   onder alle $M(\vec{p})$, op een schaaltransformatie na gelijk aan de Minkowski
   metriek.

8. Het botsingsproces waarin e^+e^- annihileren in N fotonen wordt beschreven
   door N! Feynman diagrammen die elk N-1 propagatoren van een virtueel elec-
   tron bevatten. Bij verwaarlozing van de electronmassa heeft elke propa-
   gator een singulariteit binnen de fysische faseruimte. Wanneer een gegeven
   propagator in een gegeven diagram divergeert is dit minstens ook het geval
   voor alle propagatoren tussen de eerstgenoemde en één van de uitwendige
   fermionlijnen in dat diagram.

9. Zij $f(x)$ een positieve functie en laten zowel f als de eerste twee afgeleiden continu zijn. Om de integraal van f numeriek te benaderen wordt het integratiegebiéd opgesplitst in een groot aantal intervallen waarbij in elk interval $f(x)$ benaderd wordt door een lineaire uitdrukking. Men kan de intervallen kleiner kiezen daar waar $f(x)$ groter is, zodat elk interval eenzelfde bijdrage tot de integraal levert. De opvatting dat deze benaderingswijze nauwkeuriger is dan die waarbij alle intervallen even groot gekozen worden is onjuist.